



Universidade de Aveiro Departamento de Biologia

Ano Lectivo 2014/2015

**JOANA NOGUEIRA  
RODRIGUES**

**Identificação do papel da aducina no citosqueleto  
axonal**

**Dissecting the role of adducin in the axonal  
cytoskeleton**

## **DECLARAÇÃO**

Declaro que este relatório é integralmente da minha autoria, estando devidamente referenciadas as fontes e obras consultadas, bem como identificadas de modo claro as citações dessas obras. Não contém, por isso, qualquer tipo de plágio quer de textos publicados, qualquer que seja o meio dessa publicação, incluindo meios eletrônicos, quer de trabalhos acadêmicos.



Universidade de Aveiro Departamento de Biologia

Ano Lectivo 2014/2015

**JOANA NOGUEIRA  
RODRIGUES**

**Identificação do papel da aducina no citosqueleto  
axonal**

**Dissecting the role of adducin in the axonal  
cytoskeleton**

Dissertação apresentada à Universidade de Aveiro para cumprimento dos requisitos necessários à obtenção do grau de Mestre em Biologia Molecular e Celular realizada sob a orientação científica da Doutora Mónica Sousa do Grupo de Regeneração Nervosa do Instituto de Biologia Molecular e Celular - IBMC, Porto

## **o júri**

presidente

**Professora Doutora Maria de Lourdes Gomes Pereira**  
Professor Associado com agregação, Universidade de Aveiro

orientadora

**Doutora Mónica Luísa Ribeiro Mendes de Sousa**  
Investigador principal do Instituto de Biologia Molecular e Celular - IBMC, Porto  
Nerve Regeneration Group, IBMC

co-orientadora

**Professora Doutora Sandra Isabel Moreira Pinto Vieira**  
Professor Auxiliar Convidada da Secção Autónoma das Ciências da Saúde, Universidade de Aveiro

arguente

**Doutora Ana Gabriela da Silva Cavaleiro Henriques**  
Professor Auxiliar Convidada, Universidade de Aveiro

## **agradecimentos**

Os meus agradecimentos vão, principalmente, para a minha orientadora Doutora Mónica Sousa, por me ter acolhido e ter possibilitado a realização da minha tese de Mestrado no seu grupo de investigação. Agradeço pelo voto de confiança, pela oportunidade, pela sempre disponibilidade e orientação, fornecendo todas as condições e ensinamentos necessários.

Gostava de agradecer também a todos os membros do grupo Nerve Regeneration, Rita, Raquel, Marta, Fernando, Tiago, Ana Rita, Filipa, Carolina, Sofia, Diogo e Pedro, por todo o profissionalismo, disponibilidade e ajuda em qualquer instância.

Em especial e com muito carinho, quero agradecer ao Sérgio Leite, por toda a atenção dispensada sem qualquer entrave, pela grande paciência e dedicação e pelo apoio e orientação.

À Joana, Raquel, Cris e André, pela amizade nas horas vagas desde sempre.

À Universidade de Aveiro por me ter aceite no Mestrado e me ter facilitado realizar a minha dissertação fora do estabelecimento de ensino. Em especial, à professora Doutora Sandra Vieira por se ter disponibilizado em ser minha co-orientadora durante este ano. Obrigada pelo apoio e ajuda até aos minutos finais.

E por fim, e mais importante, agradeço aos meus pais por todo o apoio e compreensão incondicional ao longo deste ano e de toda a minha vida porque sem eles nada faria sentido.

A todos, um sincero obrigada!

**palavras-chave**

Sistema nervoso, neurónio, axónio, microtúbulos, actina, proteína de ligação à actina, aducina, citoesqueleto de actina, anéis de actina, murganhos KO para  $\alpha$ -aducina, alargamento axonal, degeneração axonal, transporte axonal, modificações pós-traducionais da tubulina, motores moleculares, segmento inicial do axónio

**resumo**

O citoesqueleto neuronal é maioritariamente constituído por três componentes: actina, microtúbulos e filamentos intermédios. Com a descoberta dos anéis de actina presentes no axónio, o citoesqueleto neuronal de actina tem vindo a ganhar bastante relevância. Contudo, os mecanismos moleculares envolvidos na regulação da actina no citoesqueleto continuam por esclarecer. Nesta tese focámo-nos no estudo da importância da aducina, uma proteína de ligação à actina, na regulação do citoesqueleto neuronal. A aducina é uma proteína constituída por heterotetrameros de heterodímeros das subunidades  $\alpha/\beta$  e  $\alpha/\gamma$ , sendo que no sistema nervoso, a depleção da subunidade  $\alpha$  resulta numa completa ausência da proteína no seu estado funcional. Assim, murganhos KO para  $\alpha$ -aducina demonstraram ser um modelo animal relevante para o estudo do papel desta proteína no citoesqueleto de actina. Resultados do nosso grupo demonstraram que murganhos KO para  $\alpha$ -aducina desenvolvem uma degeneração progressiva e um aumento do calibre do axónio. Uma vez que defeitos no transporte axonal têm vindo a ser relacionados com o alargamento axonal, tornou-se importante determinar o papel da aducina no citoesqueleto axonal, mais especificamente no transporte ao longo do axónio. Apesar de não terem sido encontradas diferenças no transporte da toxina da cólera no nervo óptico, a ausência da aducina resultou num decréscimo significativo na velocidade de transporte axonal de mitocôndrias e lisossomas. Diversos distúrbios neurodegenerativos têm sido associados com deficiências no transporte axonal consequentes de alterações na maquinaria de transporte incluindo microtúbulos e proteínas relacionadas. Apesar de não terem sido encontradas diferenças nos níveis de acetilação e de-tirosinação da tubulina em amostras de cérebro  $\alpha$ -aducina KO, os níveis de tirosinação da tubulina estão significativamente diminuídos quando comparados com aqueles encontrados em amostras WT, sugerindo uma menor dinâmica dos microtúbulos na ausência de aducina. Além das modificações da tubulina, a diminuição da velocidade de transporte axonal poderá resultar também do decréscimo dos níveis de ambos os motores moleculares dineína e cinesina nos murganhos  $\alpha$ -aducina KO. Por fim, sugere-se que a aducina poderá também estar envolvida na organização e/ou plasticidade do segmento inicial do axónio dada a sua ligação ao citoesqueleto de actina, importante para a sua função e organização. Nos murganhos KO para  $\alpha$ -aducina, foi verificado que apesar da formação do segmento inicial ser normal, as células não têm a capacidade para o relocalizar após uma depolarização crónica. Porém, o papel específico da actina e das suas proteínas associadas, tal como a aducina, neste processo deverá ser investigado com maior detalhe. Sumariamente, com esta tese, foi possível contribuir para uma melhor compreensão da relevância da actina, mais especificamente, da proteína de ligação à actina aducina, na biologia de um neurónio.

**keywords**

Nervous system, neuron, axon, microtubules, actin, actin-binding protein, adducin, actin cytoskeleton, actin rings,  $\alpha$ -adducin KO mice, axon enlargement, axon degeneration, axonal transport, tubulin post-translational modifications, molecular motors, axon initial segment

**abstract**

The neuronal cytoskeleton is an interconnected network of filamentous polymers, having in its constitution three major components: actin, microtubules and intermediate filaments. Up to the discovery of axon actin rings, the neuronal actin cytoskeleton has gained relevance. Still, the molecular details of the regulation of the actin cytoskeleton in neurons are largely unknown. Helping in the actin cytoskeleton regulation and maintenance, there is adducin. Adducin is organized in heterotetramers of heterodimers which comprises  $\alpha/\beta$  and  $\alpha/\gamma$  subunits. In the nervous system, the depletion of  $\alpha$  subunit results in an almost complete absence of functional adducin. Given this,  $\alpha$ -adducin KO mice arose as relevant models to study the role of this protein in actin cytoskeleton. Results from our group showed that  $\alpha$ -adducin KO mice develop progressive axon enlargement and degeneration. As defects in axonal transport have been related to axon enlargement, we determined the importance of adducin in the axonal cytoskeleton and, more specifically, in axonal transport. Although no differences were found in the retrograde transport of CTB in the optic nerve, the lack of adducin resulted in a decreased speed of axonal transport of mitochondria and lysosomes. Several neurodegenerative disorders have been associated with axonal transport deficits and, consequently, with alterations in MT-based transport. Although no differences were found in the levels of acetylated and de-tyrosinated tubulin, the levels of tyrosinated tubulin were significantly decreased in  $\alpha$ -adducin KO brains, suggesting a less dynamic status of the MT cytoskeleton in the absence of adducin. Besides differential PTMs of tubulin the decreased axonal transport speed may result from the decreased levels of dynein and kinesin in  $\alpha$ -adducin KO mice. Lastly, we hypothesized that adducin might be involved in the organization and/or plasticity of the AIS that requires actin dynamics. In  $\alpha$ -adducin KO animals, although the AIS forms normally, neurons do not have the ability to relocate it in response to chronic depolarization. Still, the specific role of actin and its associated proteins, like adducin, in this process remains unclear. In sum, with this Thesis we contributed to understand the relevance of the actin in cytoskeleton, more specifically, of the actin-binding protein adducin in neuron biology.

# Table of Contents

Table of Contents	i
Figures List	iii
Abbreviation List	viii
Introduction	1
1. The Neuronal Cytoskeleton	1
1.1 Neuronal Polarization	3
1.2 Axon Growth	5
1.3 The Dynamics of the Actin Cytoskeleton during Axon Elongation	7
1.4 Actin Retrograde Flow	10
1.5 Actin-binding Proteins in the Neuronal Cytoskeleton	11
1.6 The Axon Initial Segment	13
1.7 Neuronal Actin Rings	14
1.8 Axonal Transport	16
2. Adducin	19
2.1 Characteristics and functions	20
2.2 Adducin and actin dynamics	21
2.3 Adducin and actin rings	23
2.4 Preliminary results: $\alpha$ -adducin KO mice develop progressive axon enlargement and degeneration	23
Objectives	26
Materials and Methods	27
Animals	27
Primary neuron cultures	27
Dorsal root ganglia neuron cultures	27
Hippocampal neuron cultures	27
Immunofluorescence	28
Adducin immunofluorescence	28
<i>In vivo</i> axonal transport assay	28
Intravitreal injection of cholera toxin B	28
Optic nerve analysis	29
<i>In vitro</i> axonal transport assay	29
Live imaging of axonal transport	29



Analysis of axonal transport and quantification _____	29
Axon initial segment assay _____	30
Immunofluorescence _____	30
Axon initial segment analysis _____	30
Western blotting _____	31
Statistical analysis _____	32
Results _____	33
I. $\alpha$ -adducin KO mice lack functional adducin tetramers. _____	33
II. The lack of adducin does not produce a significant effect in the transport of cholera toxin through the optic nerve. _____	34
III. The lack of adducin generates an impairment of the axonal transport of mitochondria and lysosomes. _____	36
IV. The absence of adducin results in decreased levels of tyrosinated tubulin and of molecular motors. _____	40
V. The lack of adducin impairs the plasticity of the axon initial segment. _____	42
Discussion _____	44
References _____	47

# Figures List

**Figure 1 – Neuronal polarization in cultured rodent embryonic hippocampal neurons.** Cells start as round spheres and, then, neuritogenesis takes place. Neuronal polarizations begins with axon formation: the break in cell symmetry that results in the elongation of one of the several neurites to form the axon. Subsequently, the other short neurites extend to form dendrites. In a final stage, neurons suffer functional maturation and develop dendritic spines. Taken from [16]..... 4

**Figure 2 – Growth cone structure.** Axonal growth occurs in the tip of a neurite and is led by a specific structure, the growth cone, which is extremely dependent on cytoskeleton dynamics and the extension of protrusive forces like filopodia and lamellipodia. The growth cone has a central domain (C-domain) where microtubules enter and transport organelles and vesicles, and a peripheral domain (P-domain) rich in actin filaments that surrounds the growth cone. The P-domain contains long, bundled actin filaments (F-actin) forming the filopodia protrusion and also a mesh-like branched F-actin networks that gives the structure to lamellipodia like-veils protrusion. Between P- and C-domain is a transition zone (T-zone), where microtubules and actin filaments interact with each other. Taken from [22]..... 6

**Figure 3 – Actin dynamics and treadmilling.** ATP binds preferentially to the barbed ends (+) of actin filaments. Subsequently, after incorporation of actin subunits, ATP is hydrolyzed into ADP-P<sub>i</sub> and then P<sub>i</sub> is released. The ATP-actin subunits are maintained at the tip of the barbed ends while ADP-P<sub>i</sub>-actin and ADP-actin are sustained in the pointed ends. This actin turnover in the two ends of an actin filament generates different monomer concentrations for assembly and disassembly creating a process called actin treadmilling. Taken from [25]..... 8

**Figure 4 – Actin retrograde flow.** The continuous movement of F-actin towards the center of the growth cone generates growth cone advancement with F-actin polymerization occurring at the leading edge (actin recycling). Adapted from [22]. ..... 10

**Figure 5 – Schematic representation of the actin-binding proteins (ABPs).** The actin cytoskeleton is regulated by several ABPs that control the nucleation, polymerization, branching and organization of the actin cytoskeleton. Adapted from [25]. ..... 12

**Figure 6 – Schematic representation of the axon initial segment (AIS).** The AIS is a specialized region where the action potential initiates, determining the efficiency of the conduction of the action potential along the axon depending on the density of sodium channels. Adapted from [33]. ..... 13

**Figure 7 – Schematic representation of axonal actin rings.** The axon cytoskeleton is composed of actin filaments capped by adducin and rearranged into rings surrounding the circumference of the axon with spectrin as a link of this network. Taken from [53]. ..... 15

**Figure 8 – Schematic representation of fast axonal transport.** The movement of organelles or vesicles along the axonal microtubules is done in the anterograde and retrograde directions. The molecular motor conventional kinesin is responsible for anterograde transport while cytoplasmic dynein generates retrograde transport. Adapted from [59]. ..... 17

**Figure 9 – Schematic representation of the molecular motor kinesin.** Kinesin heterotetramer comprises two heavy chains (the two globular heads) and two light chains connected by a long stalk. Kinesin is responsible for the anterograde transport in the axon. Adapted from [63]. ..... 18

**Figure 10 – Schematic representation of the molecular motor dynein.** Dynein comprises two heavy chains, two intermediate chains, four light intermediate chains and several light chains. Associated with dynein, there is dynactin (DCTN2 and DCTN1) helping in dynein regulation and binding capacity. Dynein is responsible for the retrograde transport in the axon. Adapted from [63]. ..... 18

**Figure 11 – Schematic representation of adducin organization.** Adducin is composed by a globular head, a neck domain required for oligomerization and a C-terminal MARCKS tail domain important to protein-protein interaction. Adducin has several phosphorylated sites represented with arrows in the figure. Taken from [86]. ..... 20

**Figure 12 – Adducin organization and regulation.** Adducin can cap the fast-growing ends of actin preventing the addition or loss of actin subunits. The phosphorylation of adducin by PKC promotes the actin-spectrin network dissociation resulting in inhibition of actin-capping activity. This allows a more dynamic state of actin. Taken from [86]. ..... 22

**Figure 13 –  $\alpha$ -adducin KO mice show progressive axon enlargement and axonopathy.** (A) Representative 12000x microphotographs of ultra-thin sections of optic nerves from WT and  $\alpha$ -adducin KO mice at P20, P60 and P100; Scale bar: 2  $\mu$ m. (B) Axon density in the optic nerve of WT (P20 n=4; P60 n=5; P100 n=5) and  $\alpha$ -adducin KO mice (P20 n=4; P60 n=5; P100 n=4) at P20, P60 and P100. (C) Representative semi-thin cross sections of WT and  $\alpha$ -adducin KO optic nerves stained with toluidine blue; Scale bar: 100  $\mu$ m. (D) Representative 6000x microphotographs of ultra-thin sections of WT and  $\alpha$ -adducin KO corticospinal tracts; asterisks highlight axons with enlarged diameter; Scale bar: 1  $\mu$ m. (E) Axon density in the corticospinal tract of WT (n=4) and  $\alpha$ -adducin KO mice (n=4) at P100. (F-G) Axon distribution according to diameter in P20 (F), P60 (G) and P100 (H) WT (P20 n=5; P60 n=4; P100 n=6) and  $\alpha$ -adducin KO (P20 n=4; P60 n=4; P100 n=5) optic nerves. (I) Representative semi-thin sections of WT and  $\alpha$ -adducin KO sciatic nerves; asterisks highlight axons with enlarged diameter; Scale bar: 10  $\mu$ m. Graphs show mean  $\pm$  SEM; p-value \* $<0.05$ , \*\* $<0.01$ ..... 25

**Figure 14 –  $\alpha$ -adducin KO mice have severely decreased levels of  $\beta$ - and  $\gamma$ -adducin and lack functional adducin tetramers.** (A) Western blot analysis of brain, spinal cord and optic nerve of WT and  $\alpha$ -adducin KO mice using a pan-specific antibody that recognizes the  $\alpha$ -,  $\beta$ - and  $\gamma$ -adducin forms [53]. (B) Anti-adducin western blot analysis of brain extracts of WT and  $\alpha$ -adducin KO brain extracts run on native gels. The 260 kDa standard is indicated (note that under reducing conditions the observed MW of an adducin dimer is of approximately 210-260 kDa [77]). (C) Western blot analysis of capping protein (ECapZ) in brain extracts of WT and  $\alpha$ -adducin KO mice. (D) Anti-adducin immunofluorescence in E16 hippocampal neurons isolated from WT and  $\alpha$ -adducin KO mice. Left panels: DAPI (blue),  $\beta$ III-tubulin (green) and pan-adducin (red); right panels: pan-adducin (white). Scale bar: 10  $\mu$ m..... 33

**Figure 15 – In vivo axonal transport analysis after CTB injection in the eye of 6 months old WT and  $\alpha$ -adducin KO mice.** (A) Representative longitudinal images of the optic nerve of WT (n=4) and  $\alpha$ -adducin KO (n=4) mice; scale bar: 1  $\mu$ m. (B) Intensity of

fluorescence along the optic nerve. The intensity of fluorescence was normalized (100% - maximum fluorescence level). The fluorescence measurements were performed from the beginning of the optic nerve (0  $\mu\text{m}$ ) to the distance of 2400  $\mu\text{m}$ . ..... 35

**Figure 16 – Analysis of the axonal transport speed of WT and  $\alpha$ -adducin KO DRG neurons.** (A-C) Quantification of the axonal transport speed of (A) mitochondria, (B) lysosomes and (C) synaptic vesicles. Graphs show mean  $\pm$  SEM; p-value \* $<0.05$ , \*\* $<0.01$ . (D-F) Upper- still images at t=0 and lower- kymographs, of (D) mitochondria, (E) lysosomes and (F) synaptic vesicles. Scale bar: time (t): 100 seconds; distance (d): 5  $\mu\text{m}$  ..... 36

**Figure 17 – Analysis of the axonal transport speed of WT and  $\alpha$ -adducin KO embryonic hippocampal neurons.** (A-C) Quantification of the axonal transport speed of (A) mitochondria, (B) lysosomes and (C) synaptic vesicles. Graphs show mean  $\pm$  SEM; p-value \* $<0.05$ , \*\* $<0.01$ . (D-F) Upper- still images at t=0 and lower- kymographs, of (D) mitochondria, (E) lysosomes and (F) synaptic vesicles. Scale bar: time (t): 100 seconds; distance (d): 5  $\mu\text{m}$  ..... 37

**Figure 18 – Analysis of the percentage of moving cargos in WT and  $\alpha$ -adducin KO DRG neurons.** Quantification of the percentage of moving (A) mitochondria, (B) lysosomes and (C) synaptic vesicles. Graphs show mean  $\pm$  SEM; p-value \* $<0.05$ . ..... 38

**Figure 19 – Analysis of the percentage of moving cargos in WT and  $\alpha$ -adducin KO embryonic hippocampal neurons.** Quantification of the percentage of moving (A) mitochondria, (B) lysosomes and (C) synaptic vesicles. Graphs show mean  $\pm$  SEM; p-value \* $<0.05$ . ..... 39

**Figure 20 – Analysis of the levels of post-translational modifications of tubulin in WT and  $\alpha$ -adducin KO mouse brains.** (A) Representative Western blot. (B-D) Quantification of the levels of (B) acetylated, (C) tyrosinated and (D) de-tyrosinated tubulin in brain tissue samples from  $\alpha$ -adducin KO and WT P30 mice. Graphs show mean  $\pm$  SEM; p-value \* $<0.05$ . ..... 40

**Figure 21 – Analysis of the levels of molecular motors in WT and  $\alpha$ -adducin KO mouse brains.** (A) Representative Western blot. (B-C) Quantification of the levels of (B)

cytoplasmic dynein and (C) kinesin heavy chain in brain tissue samples from  $\alpha$ -adducin KO and WT P30 mice. Graphs show mean  $\pm$  SEM; p-value \* $<0.05$ , \*\* $<0.01$ ..... 41

**Figure 22 – Analysis of the AIS plasticity in WT and  $\alpha$ -adducin KO embryonic hippocampal neurons.** (A) Representative images of the immunofluorescence against ankyrinG in WT and  $\alpha$ -adducin KO hippocampal neurons either under control conditions or after chronic depolarization induced by 15mM KCl; scale bar: 10  $\mu$ m. Cell bodies are surrounded by a white dashed line. The AIS is highlighted by arrowheads. (B) Analysis of the distance along the axon of the start and the end of the AIS in WT and  $\alpha$ -adducin KO hippocampal neurons either under control conditions or after chronic depolarization induced by 15mM KCl. Graphs show mean  $\pm$  SEM; p-value \*\*\* $<0.001$ ..... 42

## Abbreviation List

---

ABP	Actin Binding Protein
ADP	Adenosine diphosphate
AIS	Axon Initial Segment
AnkG	AnkyrinG
ATP	Adenosine triphosphate
BSA	Bovine serum albumin
C-domain	Central domain
CGN	Cerebellar granule neurons
CNS	Central nervous system
CTB	Cholera toxin subunit B
DAPI	4',6-diamidino-2-phenylindole, dihydrochloride
DIV	Days <i>In Vitro</i>
DMEM	Dulbecco's Modified Eagle Medium
DRG	Dorsal root ganglia
F-actin	Actin filament
FBS	Fetal bovine serum
G-actin	Globular actin
HBSS	Hanks' balanced salt solution
Hts	<i>Hu-li tai shao</i>
KCl	Potassium chloride
KHC	Kinesin heavy chain
KLC	Kinesin light chain
KO	Knock-out
MARCKS domain	Myristoylated alanine rich C-kinase substrate domain
MT	Microtubule
NaCl	Sodium chloride
NGF	Nerve growth factor
PBS	Phosphate buffered saline
P-domain	Peripheral domain
PFA	Paraformaldehyde
PKC	Protein kinase C

---

---

PLL	Poly-L-Lysine
PNS	Peripheral nervous system
SDS	Sodium dodecyl sulphate
TBS	Tris-buffered saline
TBS-T	Tris-buffered saline – 1% Tween 20
T-zone	Transition zone
WB	Western blot
WT	Wild-type

---



# Introduction

## 1. The Neuronal Cytoskeleton

Cell morphology is shaped by the cytoskeleton in order to establish cell function. The cytoskeleton is a highly dynamic network of fibers, which are constantly degraded and renewed providing structure and support to cells and to their cytoplasmic constituents. Actually, the cellular cytoskeleton can be disassembled and reassembled into different shapes according to the changing needs of the cell [1]. Despite that the name suggests a stable system, the cytoskeleton has to be very dynamic and needs a tight regulation in order to produce its function, facilitating the activity of cytoplasmic proteins and organelles. Basically, the cytoskeleton is in charge of executing and controlling cellular differentiation into specialized cell types [2].

The cytoskeleton is a link between the intracellular and the extracellular spaces being responsible for organizing intracellular transport and cell polarity. This connection is possible due to the fact that its components are efficiently regulated allowing a quick cell response to external mechanical or chemical signals [1, 2]. Even in plants or fungi, despite the presence of a cell wall, the cytoskeleton is extremely important [3].

The cytoskeleton in eukaryotic cells is an interconnected network of filamentous polymers, having in its constitution three major components: microfilaments, microtubules and intermediate filaments. Each one has a very specific composition and cell organization. For that reason, all these polymers have the capacity to control the mechanics of an eukaryotic cell by arranging and maintaining the integrity of the intracellular compartment [4]. Microtubules (MTs) are the largest type of filament (25 nm) and they are polarized polymers made of  $\alpha/\beta$ -tubulin heterodimers [4]. These filaments are responsible for separating chromosomes and for the transport of large particles in eukaryotes [3]. Microtubules have the most complex assembly and disassembly dynamics. They are capable of switching their conformation passing from stably growing to rapidly shrinking. This switching dynamics provides a fast reorganization of the microtubule cytoskeleton [1]. Intermediate filaments are a group of polymers not polarized that do not have the capacity to support directional movement. As expected by their name, they have an intermediate diameter and they function as ligaments in cells making them resistant to mechanical forces [3]. Neurofilaments are neuron-specific intermediate filaments that regulate the cytoskeleton and axonal transport [5].

Microfilaments are the smallest type of filament (5-7 nm) and they are composed of actin, capable of extending along the cell providing protrusive and contractile forces [4]. These filaments are less rigid than microtubules and they are in charge of supplying structure and motility [1]. In contrast, actin filaments do not change their stages of polymerization as dynamically as microtubules. These filaments are formed by polymerization of monomers of globular actin (G-actin) creating filaments of actin (F-actin) [4]. Actin filaments can create a number of linear bundles involved in supporting protrusions which are associated with cell-to-cell communication [1]. The actin filament is the dominant cytoskeletal protein playing a crucial role in maintaining cell morphology and organization, being the essential key for the survival of most cells [2].

The main differences that distinguish the three major cytoskeletal polymers are their mechanical rigidity, the dynamics of their assembly, their polarity and the type of molecular motors they are associated with [1]. Furthermore, actin filaments and microtubules are very efficient in the conversion of molecular signals into mechanical changes in order to modulate cell shape [6]. Actin and microtubule polymerization and depolymerization provide the cytoskeleton forces needed to direct the cell's movement together with molecular motors that move along with cytoskeleton components [1].

As so many cellular functions depend on the cell's cytoskeleton it is easy to understand that abnormal regulation or deficiencies in its components can lead frequently to several diseases or pathologies in humans, including cancer, neurological disorders or cardiomyopathies [7]. Promising studies have shown an association between neurodegenerative disorders and cytoskeleton dysfunction, more precisely in cytoskeleton constituents involved in vesicular transport and synaptic signaling [8]. Thus, defects in the cellular cytoskeleton may be an important cause of neurodegeneration.

In this Thesis, we will mainly focus on the analysis of the neuronal cytoskeleton.

The nervous system is a complex network of communication that can be divided into two major systems: the central nervous system (CNS) formed by the brain and the spinal cord, that is responsible for processing information, and the peripheral nervous system (PNS) formed by nerves and ganglia which are in charge of propagating the information received into the CNS [4]. The nervous system is constituted by specialized cells, the neurons, which are capable of transferring rapidly information from one part of the body to another. Neurons are unique. These cells coordinate the body's activity receiving stimuli from outside and inside of the body and sending this information to other parts of the organism like muscles or glands [4]. They are capable of responding effectively and rapidly to several types of cell signaling, integrating and regulating the

information in order to transmit it over long distances by electrical impulses [9]. Neurons are constituted by a cell body (or soma) with a nucleus and neuronal processes called neurites, which may become dendrites or axons, essential components for the development of a functional neuronal network [5].

The axonal and dendritic surfaces play important roles in message receiving, processing and propagation, together with other specialized regions in the plasma membrane such as the cell body, dendritic shaft, axon shaft, axon initial segment, nodes of Ranvier and presynaptic terminals [9]. As detailed below, the specification of the nervous system and the control a number of different neuronal functions is tightly regulated by the neuronal cytoskeleton.

## **1.1 Neuronal Polarization**

Neurons, as signaling cells of the nervous system, are the best characterized polarized cell type in the human body. Mammalian neurons usually migrate over long distances before reaching their final destination and they undergo axon-dendrite polarization during migration, which is dependent on the actin filaments and microtubules that exist in cytoskeleton. Both have an important function in terms of establishing cell polarity, crucial to the function of diverse cell types and even more to specific cells like neurons [2].

Neuronal polarization forms the basis for signal propagation allowing neurons to segregate signals and transmit them to distinct sites [10, 11]. Primary cultures of dissociated rodent embryonic hippocampal neurons (embryonic day 18 [E18]) are one of the most used neuron types as model system to study neuronal polarity, together with postnatal cerebellar granule neurons (CGN, postnatal day 4-10) [9, 12, 13]. There are specific events of neuronal differentiation that can be divided into different stages and all of them are associated with characteristic morphological changes (figure 1) [5]. During neuronal polarization the neuron gives rise to two morphological and functional compartments: a thin and long axon and several shorter dendrites [14]. All neurons start as small apolar symmetric spheres that, after plating, can attach to a substrate (stage 1) [9, 12-16]. Then, neurites start to extend. Neurite formation, known as neuritogenesis, requires cytoskeleton regulation [11], which suggests that neurites have a very dynamic cytoskeleton in their tips [9, 12]. The formation of a neurite starts with the establishment of an enriched actin network in the neuronal cell body [5]. At this phase, neurons are able to

extend 4-5 neurites (stage 2 – 12 to 24 hours after plating) [9, 12, 15, 16]. Up until here, neurons are still unpolarized cells with a symmetric structure [14]. Neuronal polarization starts with axon formation: the break in cell symmetry that results in the elongation of one of the several neurites into a long neurite to become the axon [2, 10, 15, 16] (stage 3 – 24 to 48 hours after plating). At this stage, the other neurites halt their growth [9]. Only after a few days (stage 4 - 3 to 4 days in culture) the other short neurites extend to form dendrites that are responsible for connecting to other neurons leading to another important change in cell morphology [2, 11, 16]. When neuronal signaling happens, dendrites receive signal input from other neurons that are processed in the cell body and propagated over the axon to the presynaptic terminals (stage 5 – 1 week in culture) [9, 12, 15, 16]. Here, synapses are formed together with other neurons' dendrites [2]. After one week in culture, neurons suffer functional maturation and start to develop dendritic spines (stage 6) [9, 15, 16].

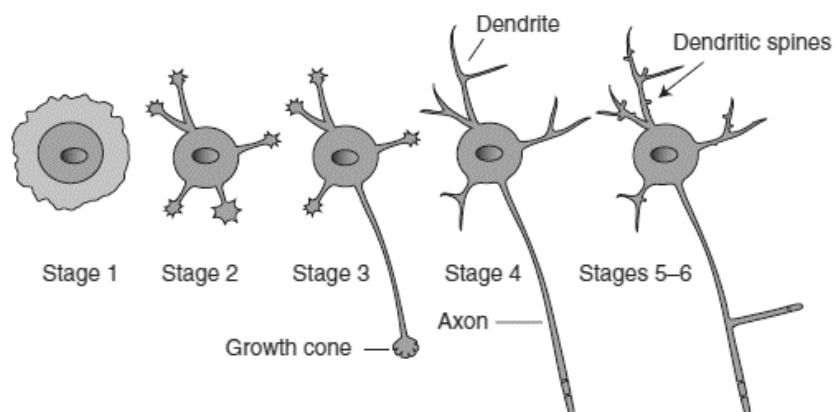


**Figure 1 – Neuronal polarization in cultured rodent embryonic hippocampal neurons.** Cells start as round spheres and, then, neuritogenesis takes place. Neuronal polarization begins with axon formation: the break in cell symmetry that results in the elongation of one of the several neurites to form the axon. Subsequently, the other short neurites extend to form dendrites. In a final stage, neurons suffer functional maturation and develop dendritic spines. Taken from [16].

It is still not clear why one of the minor neurites is capable of elongating into an axon and the others remain shorter dendrites. But it is known that there are some cell signals sensed by neurites at stage 2 that promote axon formation [9]. Although all neurites are capable of sensing these signals, the chosen neurite produces “growth-discouraging signals” that culminate in its faster growth when compared to the neighboring neurites [9].

It is important to note that even upon lesion of the original axon, at stage 3, neurons have the capacity to “choose” another neurite to extend and become the axon [9, 15]. Neurons are able to elongate processes with axonal morphology in preexisting dendrites one day after injury and axotomy (cutting the axon) can induce changes in a mature cell in a similar way that happens, initially, in an immature cell [17]. Also, if after axotomy, the cut axon remains longer than the other neurites (dendrites), it can still regenerate and form the axon [18].

The elongation of the future axon and extension of neurites into dendrites are stages needed to identify how neurons become polarized [2]. Asymmetric organization and signaling cascades are the two main processes required for maintenance of polarization [14]. And, certainly, axon formation is the key to establish neuronal polarity.

## **1.2 Axon Growth**

Axon formation acts like a decision event for neuron polarization starting with the extension of one of the neurites to develop the long axon whereas the short neurites extend to form short dendrites [11]. Consequently, neurons must have a robust mechanism that guarantees this generation of one, and only one, axon [18].

Axon growth is lead by changes in the tip of a neurite in a structure known as the growth cone (figure 2), a structure rich in actin filaments with a concentration of 100  $\mu\text{M}$ , which is much higher than the one that is necessary for actin polymerization (about 0.1  $\mu\text{M}$ ) [19]. The growth cone is extremely dependent on actin cytoskeleton dynamics, allowing the extension of protrusive forces by neurons in order to form the future axon [20, 21]. Neurons are able to extend two protrusive forces: filopodia and lamellipodia. Lamellipodia are broad veil-like protrusions that function as sensors of the environment outside the cell contributing to neuron cell motility and adhesion, while filopodia are thin extend processes that amplify the extracellular area allowing the cell to detect signals [16, 21]. Filopodia may also have an important role in establishing adhesive contact with substrates promoting the substrate's attachment [22]. Although structurally distinct, both filopodia and lamellipodia are shaped by F-actin [21]. The sensory functions of filopodia and lamellipodia are extremely important to the advance of the growth cone which depends on the dynamic assembly and disassembly, organization and turnover of actin filaments [19]. Still, the mechanisms that lead to the formation of these forces by the cell or that coordinate the actin filaments in the cell body remain unclear [5].

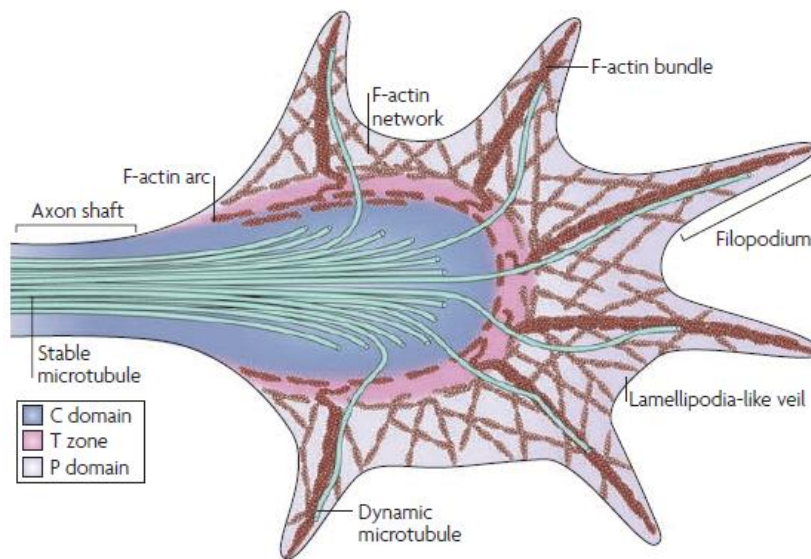


**Figure 2 – Growth cone structure.** Axonal growth occurs in the tip of a neurite and is led by a specific structure, the growth cone, which is extremely dependent on cytoskeleton dynamics and the extension of protrusive forces like filopodia and lamellipodia. The growth cone has a central domain (C-domain) where microtubules enter and transport organelles and vesicles, and a peripheral domain (P-domain) rich in actin filaments that surrounds the growth cone. The P-domain contains long, bundled actin filaments (F-actin) forming the filopodia protrusion and also a mesh-like branched F-actin networks that gives the structure to lamellipodia like-veils protrusion. Between P- and C-domain is a transition zone (T-zone), where microtubules and actin filaments interact with each other. Taken from [22].

The growth cone has a central domain (C-domain), a region connected to the axon shaft, with a high density of microtubules transporting several organelles and vesicles along the axon [2, 23]. Microtubules enter from the axon shaft providing structure and rigidity to this neurite, and are polymerized in their growing ends towards the leading edge [14]. The growth cone has also a peripheral domain (P-domain) rich in actin filaments that surrounds the cone [2, 24]. The P-domain is enriched in actin and consequently responsible for filopodia and lamellipodia formation, resulting in a network of branched actin filaments [16]. Actin filaments present in the growth cone create an actin corridor between these two regions [22]. Between the P- and C-domain, there is a transition zone (T-zone), where microtubules and actin filaments interact with each other [21]. This T-zone plays a role in actin and microtubule regulation in the growth cone, more specifically, in monitoring the actin flow in the P-domain [23]. The majority of microtubules are present

in the C-domain but single microtubules can cross this region to the T-zone in order to interact with actin filaments [23].

The process of growth cone advance and progression can be divided in three stages: protrusion, engorgement and consolidation [23], and these steps are constantly being repeated [2]. In the first step, there is a contact between the distal part of the growth cone and an adhesive substrate. This binding promotes the activation of several receptors which leads to the interaction between the substrate and the P-domain actin cytoskeleton [23]. The P-domain forms both protrusive processes: filopodia to elongate and lamellipodia to move forward. Here, actin filaments are incorporated as globular actin, promoting a continuous actin polymerization [2]. Whereas lamellipodia contain branched actin filaments, filopodia are constituted by unbranched actin filaments [16]. Consequently, in the engorgement phase, actin filaments generate a F-actin corridor creating the cytoplasm's movement [2]. Basically, actin polymerization forces the elongation of filopodia towards F-actin allowing the creation of new intracellular space in order to permit the advancement of the cytoplasm in the direction of the site of new growth, monitored by the entering of microtubules which are guided by the T-zone [22]. Like filopodia, lamellipodia is elongated at the same time and supported by actin polymerization being a requirement for lamellipodia extension [21]. If, for some reason, actin filament polymerization is stopped or even blocked, this extension process is immediately halted [21]. Finally, in consolidation, axon extension is over when the termination of protrusive forces from the sides of the advancing growth cone occurs and the P-domain is transformed into the central body of the growth cone (C-domain) [23]. As a result, there is a polarized structure at the tip of the axon [21].

### **1.3 The Dynamics of the Actin Cytoskeleton during Axon Elongation**

The assembly and disassembly of actin plays an essential role in growth cone motility and the increase of actin dynamics determines which process becomes the axon [19]. Instability of actin filaments causes actin disassembly allowing an increase in intracellular vesicular transport and promoting the extension of microtubules into the axon [18].

In cells, actin can exist in two simple shapes: monomeric or filamentous. Actin polymerization and, consequently, new filament formation, starts with the transition of its monomeric form (globular actin) to its filamentous form (actin filaments). Actin is an

ATPase and ATP hydrolysis is the main regulatory process responsible for this transition as actin polymerization levels may be correlated with ATP or ADP association [7, 22]. So, ATP binds globular actin in order to polymerize it and form helical actin filaments. Then, actin hydrolysis occurs and, subsequently, the dissociation of the phosphate present in ATP [10]. ATP is generally spontaneously added to the barbed fast growing end (plus (+) end) of actin leading to the growth of F-actin (actin polymerization), while the dissociation of the filament occurs in the pointed slower growing end (minus (-) end) by disconnection of ADP to G-actin (actin depolymerization) [7]. This generates a process called actin filament treadmilling (figure 3).

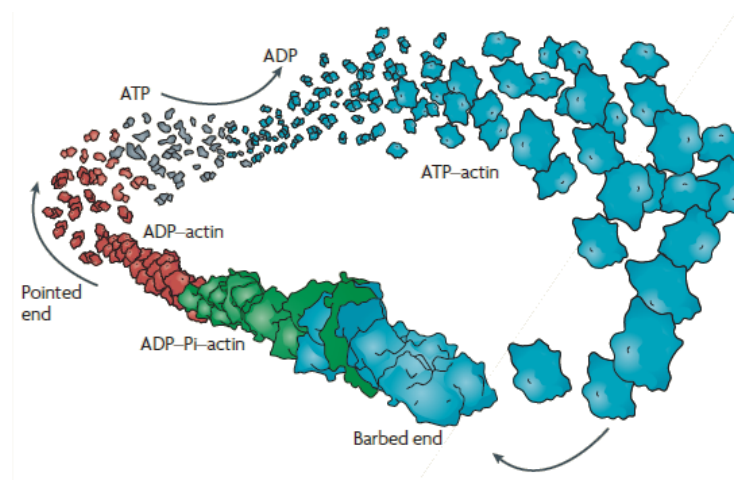


**Figure 3 – Actin dynamics and treadmilling.** ATP binds preferentially to the barbed ends (+) of actin filaments. Subsequently, after incorporation of actin subunits, ATP is hydrolyzed into ADP-P<sub>i</sub> and then P<sub>i</sub> is released. The ATP-actin subunits are maintained at the tip of the barbed ends while ADP-P<sub>i</sub>-actin and ADP-actin are sustained in the pointed ends. This actin turnover in the two ends of an actin filament generates different monomer concentrations for assembly and disassembly creating a process called actin treadmilling. Taken from [25].

Polymerization of actin monomers into stable filaments starts very slowly due to the fact that globular actin is very unstable. However, as actin polymerization starts, it is an efficient and fast process. When polymerized, all actin filaments point in a similar direction with faster growth in one end and slower in the other [3].

There are two models explaining actin dynamics during axon initiation: the convergent elongation model and *de novo* nucleation model. The convergent elongation model is explained by the elongation of the branch of actin filaments formed by the Arp2/3 complex that results in the extension of the neurite. In other hand, the *de novo* nucleation



model proposes the formation of neurites by factors that lead to actin nucleation and actin filament elongation in a single direction [5, 26].

In the growth cone, there are significant changes in actin dynamics resulting in a more unstable cytoskeleton and in an increase of actin instability [6]. There, the cytoskeleton becomes highly dynamic given the polymerization of actin filaments that become less condensed [21]. This process does not happen in other neurites. This is the reason why microtubules cannot easily enter the growth cone of dendrites. Here, there is a rigid barrier formed by condensed actin filaments retaining a dense meshwork when compared with the axon [14]. In dendrites, there is more stable actin than in the growth cone of the future axon [6]. The actin cytoskeleton dynamics that exists in the axon provides the advance of microtubules into the P-domain stimulating axon extension [14]. Therefore, the neurite with the most active growth cone becomes the neuron's axon [6].

At the growth cone, filopodia have been shown to regulate the advance of lamellipodia [21]. The two processes, filopodia and lamellipodia, are supported by an actin cytoskeleton and both show similar behaviors characterized by cycles of extension and retraction that promote the advance of one specific neurite in order to form the axon [2]. However, they are structurally different. Filopodia are organized in F-actin where the barbed ends point directly to the tip of the axon. This organization allows for a specific correlation between the direction of actin filaments and the tip of the protrusive force, which seems to be generated towards F-actin [21]. Lamellipodia are formed by G-actin which directly affects the lamellipodia formation since it is localized in leading edges of protrusion [7, 27]. However, the actin turnover can vary in both forces. The turnover of actin filaments is slower in filopodia when compared with lamellipodia. This can be explained by the fact that in filopodia there is some sort of transport of proteins and/or vesicles which may be accomplished by a more stable structure reflecting the need for a less dynamic organization of the cytoskeleton to support this specific force [21].

The cytoskeletal dynamics defines the elongation of the growth cone resulting in the movement of the cytoplasm into protrusive structures including some of the cytoskeleton constituents like microtubules and organelles. It has been demonstrated that although filopodia protrusion is what causes the tension needed to initiate neurite elongation, this force is not able to induce movement of the growth cone or even of a neurite all by itself, suggesting that microtubules also support neurite elongation [17]. In fact, differences in stability of acetylation and tyrosination of microtubules are found in axons and dendrites even in initial stages of neuronal polarization suggesting also the importance of microtubule stabilization in axon differentiation [17].

This actin regulation, together with microtubule dynamics, is crucial to axon elongation and growth cone motility, more specifically, to modulate growth cone velocity and direction [25].

## 1.4 Actin Retrograde Flow

As actin polymerization occurs, there is some membrane tension that pushes the actin filament network backwards. This is known as actin retrograde flow [21] (figure 4).

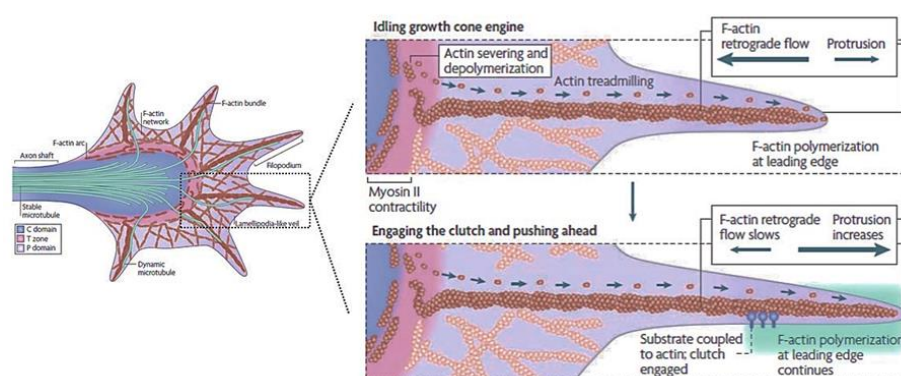


**Figure 4 – Actin retrograde flow.** The continuous movement of F-actin towards the center of the growth cone generates growth cone advancement with F-actin polymerization occurring at the leading edge (actin recycling). Adapted from [22].

This actin retrograde flow, the movement of F-actin from the leading edge towards the center, is what gives the growth cone the capacity to move [22]. With the fast growing ends pointing towards the distal membrane, polymerization of actin can generate a force that simply pushes actin network backwards [14]. This process occurs in the P-domain and is caused by the interaction between actin filaments and the contractility myosin motor molecules [22]. Myosins are the motor molecules responsible for the binding to F-actin and movement of cargos and there are several myosins participating in motility of the growth cone. Motor myosin II is the most abundant myosin in the P-domain pulling the actin back from the leading ends and recycling G-actin. Lastly, the accumulation of myosin II in the growth cone P-domain is what stops the microtubules to advance into the growth cone of the future axon [19].

## 1.5 Actin-binding Proteins in the Neuronal Cytoskeleton

The actin cytoskeleton is a highly dynamic structure regulated by a large number of actin-binding proteins (ABPs) that control the nucleation, polymerization, branching and organization of the actin cytoskeleton. Several ABPs function as actin regulators controlling actin polymerization and depolymerization [19]. ABPs can sequester actin subunits modulating the pointed and barbed end addition or dissociation of actin monomers [7].

ABPs are able to reorganize actin filaments according to the changing needs of neurons and this can influence cell morphology, in particular, the shape of filopodia and lamellipodia [19, 26]. Lamellipodia are regulated by the Arp2/3 complex [16, 19]. The Arp2/3 complex is an actin-nucleating complex that is capable of binding at the side of an existing actin filament and nucleate new filaments, resulting in a branched actin filament [19]. The specific function of the Arp2/3 complex remains unclear but it is known that lamellipodia formation is dependent on the specific levels of this complex [5]. When actin filaments are capped by other proteins, more G-actin is available for Arp2/3 nucleation and this results in the formation of branched actin instead of actin filament elongation [5]. On the other hand, formins, together with anti-capping protein, allow actin polymerization which is essential for filopodia protrusion [28]. Formins are able to capture actin monomers and nucleate them remaining bound to the actin barbed end in order to facilitate polymerization [19]. Essentially, formins can mediate the assembly of unbranched actin filaments [7]. Both Arp2/3 and formin bind profilin improving actin monomer availability for nucleation, stimulating actin filament assembly [25].

Besides actin nucleator proteins, there are other regulatory proteins that can directly affect growth cone dynamics through the interaction with actin, including several capping proteins. Capping actin barbed ends is an important process of actin regulation and organization. The most common capping protein is CapZ, which is able to bind to free actin ends and prevent the addition or loss of actin subunits [23]. A capping protein can bind to the actin barbed ends, capping them, and blocking actin growth [25]. This elongation block is crucial to promote lamellipodia protrusion in order to increase the levels of G-actin to be polymerized [23]. So, the availability of free F-actin barbed ends is regulated by capping proteins that, when linked to actin, block the addition of new monomers [19]. Besides that, actin depolymerizing factor (ADF)/cofilin are other members of the actin-binding protein family which promote the pointed-end depolymerization of actin filaments [23]. These proteins are responsible for the continuous disassembly of actin [5]. ADF/cofilin in excess can promote actin filament breakdown [19]. It is important

to note that there is a balance between cofilin and profilin that is crucial to neuronal dynamics, to prevent uncontrolled actin polymerization [10]. Cofilin releases G-actin for polymerization by profilin, an ABP that enhances the binding of G-actin monomers that are being incorporated into barbed ends [10, 16, 29]. So, profilin promotes actin polymerization while cofilin promotes actin depolymerization [16]. The actin cytoskeleton is also regulated by Ena (enabled)/VASP (vasodilator stimulated phosphoprotein) [5, 30]. These proteins, localized in filopodia and lamellipodia tips, can lead to the growth and extension of actin filaments at the membrane through its anti-capping activity, preventing the binding of capping protein to actin and allowing filament elongation [10]. Furthermore, this protein can recruit profilin. However, the relevance of this connection is not fully understood [16]. Another essential group of proteins that actively participate in actin dynamics is the WAVE (Wiskott-Aldrich Syndrome Protein [WASP]-family verprolin-homologous protein) complex. This complex is localized in lamellipodia and regulates actin polymerization together with Arp2/3 complex [31].

All of these actin regulatory proteins have specific control functions of actin cytoskeleton dynamics and several evidence show the importance of the balance that must exist between them in order to establish an efficient neuronal actin cytoskeleton (figure 5).

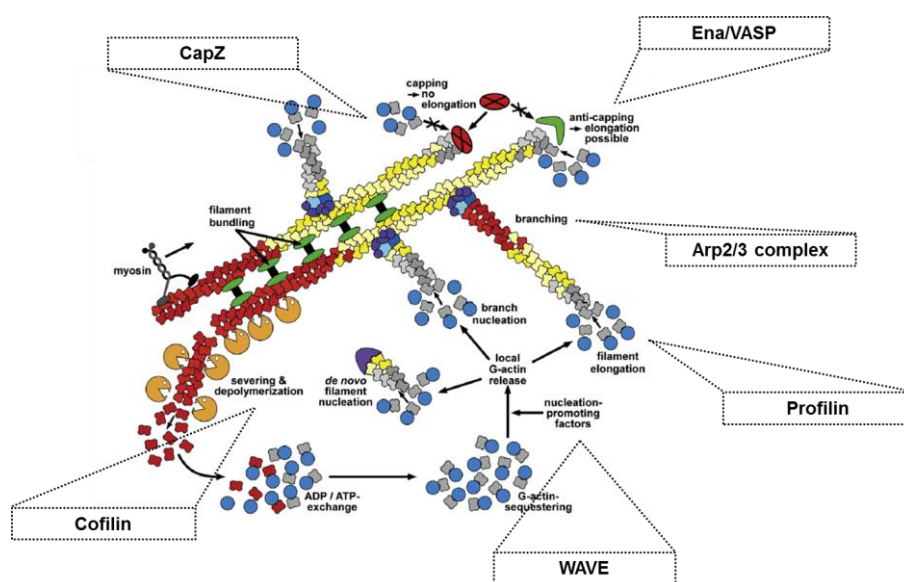


**Figure 5 – Schematic representation of the actin-binding proteins (ABPs).** The actin cytoskeleton is regulated by several ABPs that control the nucleation, polymerization, branching and organization of the actin cytoskeleton. Adapted from [25].

## 1.6 The Axon Initial Segment

The nervous system is responsible for generating and propagating action potentials. Neurons can receive excitatory signals in their cell bodies or dendrites and the axon can transmit the action potential passing the stimulus until it reaches the axon terminal [32, 33]. As the action potential reaches the pre-synaptic terminals, neurotransmitters are released in order to promote the transmission of the stimulus to other cell(s) [32].

Near the start of the axon, there is a specialized region where the action potential initiates, a region known as the axon initial segment (AIS) [34] (figure 6).

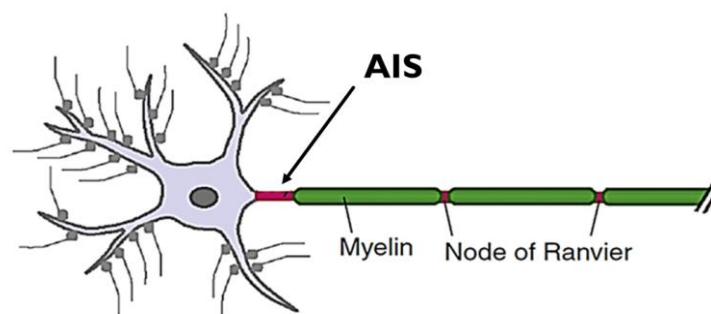


**Figure 6 – Schematic representation of the axon initial segment (AIS).** The AIS is a specialized region where the action potential initiates, determining the efficiency of the conduction of the action potential along the axon depending on the density of sodium channels. Adapted from [33].

The AIS is localized between the axon hillock and the first segment of myelination, occupying the first 10-60  $\mu\text{m}$  of the axonal length [35, 36]. The AIS separates the somatodendritic domain from the axonal domain. This area of the axon determines the efficiency of the action potential conduction along the axon depending on high densities of voltage gated sodium channels [36-39], similarly to what happens at the nodes of Ranvier [32]. So, nodes and AIS have identical physiology and organization consistent with the fact that these two structures have similar functions [34]. It is known that the spike initiates in the AIS because threshold voltage is significantly lower in this region, when compared with the rest of the axon [35, 40]. Cytoskeletal proteins like ankyrin G (ankG) and  $\beta\text{IV}$  spectrin are required to mediate the action potential efficiently since the ion channels present at the AIS (and at the nodes of Ranvier) are dependent on the binding of these scaffolding proteins [34, 41-45].

Concentrations of specific ions like sodium ( $\text{Na}^+$ ), potassium ( $\text{K}^+$ ) and calcium ( $\text{Ca}^{2+}$ ) are necessary to regulate and determine the spike generation [35] which suggest

that the AIS could easily be affected by changes or deficiencies in these ion levels allowing the development of several diseases [45]. For example, changes in electrical activity lead to alteration of the position of the AIS in neurons [39, 45, 46]. It seems that neurons are able to modify the axonal location of the AIS to respond to changes in electrical activity [45]. According to [39], chronic depolarization induced by increasing extracellular potassium levels leads to an increase in excitatory drive and the AIS moves distally away from the soma in order to decrease this neuronal excitability.

The exact location of the AIS has significant consequences for neuronal polarity and can be influenced by actin organization [35, 47]. Actin is highly enriched in the AIS and the AIS function depends on actin cytoskeleton dynamics [48]. Several experiments have shown that vesicles that carry dendritic proteins can enter either in axons or dendrites with equal frequency, but once inside the AIS, these vesicles stop or reverse their transport. This disruption in transport is dependent on actin and myosin. Oppositely, vesicles that carry axonal proteins can move efficiently along the axon [49]. An actin-dependent barrier is thought to be created in the AIS in order to mediate vesicle transport, allowing the passage of vesicles carrying axonal proteins and blocking the ones that carry dendritic proteins [50]. The formation of this barrier is what allows the separation between the components of axons and dendrites [51, 52].

Although the AIS is thought to be crucial for a functional neuron, the mechanisms underlying its composition, organization and formation are not fully understood. It is known that the location of the AIS can vary across different neuronal types [34], but the factors that determine its precise position in individual neurons, or even how the axonal translocation of the AIS happens, are still unclear.

## **1.7 Neuronal Actin Rings**

The neuronal cytoskeleton is characterized by the presence of high levels of actin filaments, playing a crucial role in maintaining cell morphology and in establishing cell polarity. However, the presence of these actin filaments and its organization along the axon is not fully understood. Recently, findings using super resolution microscopy, proposed a new model for the organization of the axonal actin cytoskeleton. Apparently, actin filaments are organized in actin rings around the circumference of the axon with a periodicity of approximately 190 nm, suggesting the presence of a compound that connects these structures of actin [53-55] (figure 7). The protein spectrin was suggested

to be the linker in this network since spectrin tetramers have, approximately, 150 to 250 nm in length [53]. Spectrin is an actin filament binding protein which is responsible for the structure of the cell and protection of the axon cytoskeleton from mechanical damage providing stability to neurons and allowing an efficient balance in pre-synaptic terminals [41, 56, 57].

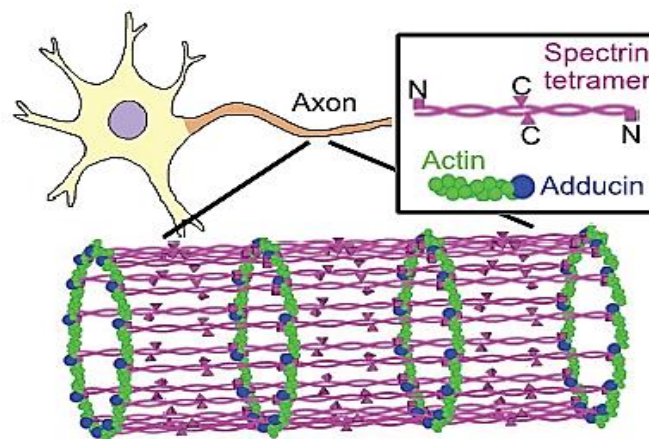


**Figure 7 – Schematic representation of axonal actin rings.** The axon cytoskeleton is composed of actin filaments capped by adducin and rearranged into rings surrounding the circumference of the axon with spectrin as a link of this network. Taken from [53].

Spectrin is found in rings forming an alternating pattern with actin rings along the axon. Disassembly of the actin rings also causes the disassembly of the spectrin rings [54, 55]. Besides, knocking-down spectrin leads to loss of actin distribution [55]. So, actin and spectrin pattern organization is interdependent suggesting a connection between actin rings and spectrin tetramers [55]. Axonal actin rings start to appear at the developmental stage 3, at DIV2, when the brake of symmetry occurs, becoming completely clear at DIV7 and maintained in older neurons (DIV28) [53], which is consistent with the fact that ring formation occurs after axon specification and growth [55]. Recently, actin rings were shown to be present not only in axons but also to be part of the submembraneous cytoskeleton in dendrites [58].

Besides spectrin, there are other proteins helping in actin ring organization such as adducin [53]. Adducin is a protein that caps the growing end of actin promoting the binding of spectrin to the rings. So, actin filaments are capped by adducin and arranged into a ring structure along the entire axon [53, 55].

It is essential to comprehend how extracellular signals regulate the axonal actin rings and how these rings are formed along the axon. In the other hand, understanding what determines the formation of actin rings is crucial to identify the differences in the organization of actin filaments depending on axon components and molecules.

## **1.8 Axonal Transport**

Several cargos, such as membranous organelles, synaptic vesicles, signaling molecules, growth factors, proteins, cytoskeletal components or even ion channels, localized in the cell body, are transported along the axon cytoplasm [59, 60]. Axonal transport can be done in two ways: anterograde and retrograde direction. The first implies the movement from the neuronal cell body along the axon while the second involves the movement towards the cell body [59]. Besides that, transport along the axon can vary through transport rates. In other words, there is fast and slow axonal transport [61, 62]. Fast axonal transport is bidirectional which means that proteins can be distributed by fast anterograde transport and return to the neuronal soma by fast retrograde transport [59]. The fast transport is responsible for the movement of proteins preassembled as membranous organelles such as vesicles, and organelles including mitochondria or even proteins stored in the lumen of these organelles. Although proteins can move in both directions, each particle prefers to move in a singular way [63]. Oppositely, proteins can also be transported in a slow rate resulting in slow axonal transport which is the case of some cytoskeletal proteins, like microtubules and neurofilaments [61].

The first stage of axonal transport includes synthesis, sorting and packaging of organelles and after that, there is a connection with the transport machinery which includes the addition of an appropriate motor molecule [59]. So, an active axonal transport is done by specific enzymes that can use ATP energy in order to promote ATP hydrolysis and generate movement along the cell [64]. Molecular motor proteins like dynein and kinesin perform this axonal transport, more specifically the retrograde and anterograde transport, respectively. Kinesin and dynein are microtubule-dependent motors that move sideways with microtubules along the axon according to the intrinsic polarity of the filaments [65, 66] (figure 8).



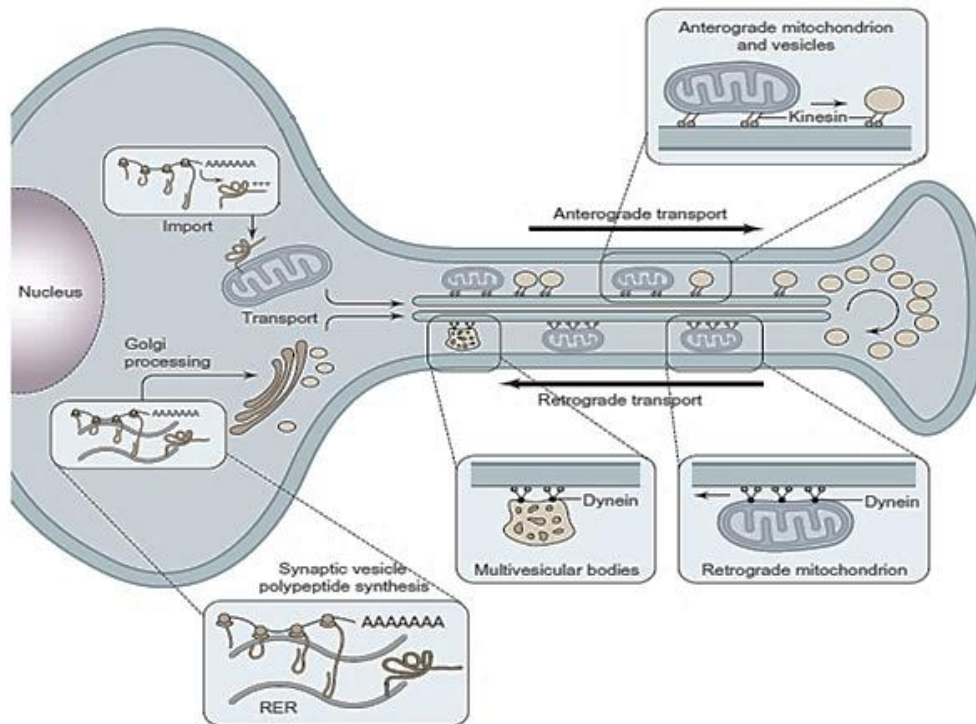


**Figure 8 – Schematic representation of fast axonal transport.** The movement of organelles or vesicles along the axonal microtubules is done in the anterograde and retrograde directions. The molecular motor conventional kinesin is responsible for anterograde transport while cytoplasmic dynein generates retrograde transport. Adapted from [59].

Conventional kinesin is the most well-known member of the kinesin family and it was the first axonal transport molecule being identified [67]. This rod shaped protein is a heterotetramer that comprises two heavy chains (115-130 kDa) and two light chains (62-70 kDa) [59, 64, 66] (figure 9). Kinesin, also known as kinesin-1 or KIF, has two globular heads, composed by the two kinesin heavy chains (KHC). These KHC contain the motor domain of the protein binding to microtubules and hydrolyzing ATP [62]. Kinesins are generally plus-end-directed motor proteins and since microtubules have their plus ends oriented towards the distal end of the axon, kinesin in the axon moves with an unidirectional transport, more specifically in an anterograde way [60, 66]. Kinesin also has a fanlike tail connected to heads by a long stalk where kinesin light chains (KLC) are localized [59, 62].

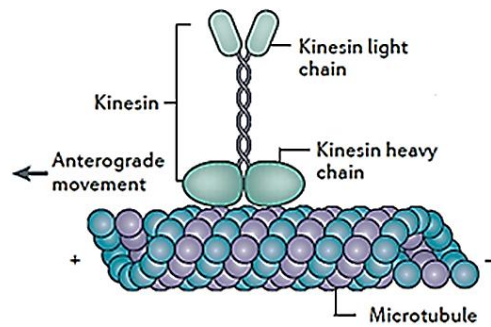


**Figure 9 – Schematic representation of the molecular motor kinesin.** Kinesin heterotetramer comprises two heavy chains (the two globular heads) and two light chains connected by a long stalk. Kinesin is responsible for the anterograde transport in the axon. Adapted from [63].

The dynein family comprises two groups: cytoplasmic dynein and axonemal dynein, also known as flagellar dynein [62]. Cytoplasmic dynein is, like kinesin, a holoenzyme with a high molecular weight comprising two heavy chains (520 kDa), two intermediate chains (74 kDa), four light intermediate chains (33-59 kDa) and several light chains (10-14 kDa), forming a complex with approximately 1 500 kDa [62] (figure 10). The heavy chains have ATP activity and MT binding domains [63]. Dynein is known to be a minus end-directed motor protein, which suggests that this protein is, in fact, the molecular motor responsible for retrograde transport [60, 68]. Cytoplasmic dynein is responsible for the transport of misfolded proteins for degradation being essential for an effective retrograde axonal transport [68]. Besides that, dynein is associated with an important protein called dynactin that regulates dynein activity through its binding capacity [62].

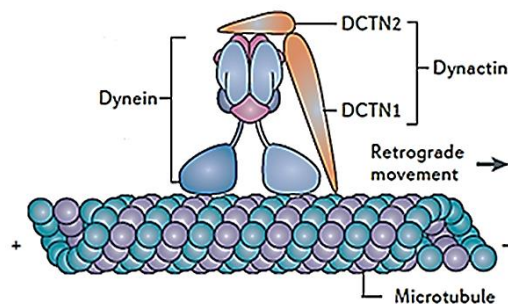


**Figure 10 – Schematic representation of the molecular motor dynein.** Dynein comprises two heavy chains, two intermediate chains, four light intermediate chains and several light chains. Associated with dynein, there is dynactin (DCTN2 and DCTN1) helping in dynein regulation and binding capacity. Dynein is responsible for the retrograde transport in the axon. Adapted from [63].

Axons, in humans, can reach one meter of length or even more, which supports the importance of an efficient and regulated transport of materials. Defects in axonal transport have been related to neurodegeneration and several human degenerative disorders like Alzheimer disease, Huntington disease or Amyotrophic Lateral Sclerosis, and this could be the result of disruptions in several proteins and components transported or in the machinery required for axonal transport [60, 64, 66]. For example, loss of kinesin heavy chain function results in an hereditary form of spastic paraplegia, a disease described by a progressive dysfunction and degeneration of upper motor neurons [59]. Similarly, mutations in dynein also result in degeneration. For example, dynein heavy chain mutations lead to defects in the sensory system in mammals [59].

## **2. Adducin**

In the sub-membraneous skeleton, the major component is spectrin [69], an extended rod-shape protein that connects with other members of the actin cytoskeleton. The erythrocyte membrane skeleton is the best characterized and the first example of the spectrin-actin interaction [70]. This spectrin-based membrane skeleton is very important to maintain the stability and support the cell membrane allowing an efficient organization of proteins in specific domains and regulation of vesicle interaction [71]. Fundamentally, the spectrin-based membrane skeleton is formed by spectrin tetramers involving  $\alpha$ -spectrin and  $\beta$ -spectrin heterodimers [72, 73]. The spectrin-actin cytoskeleton comprises several proteins. Scaffolding proteins like ankyrin and 4.1 have affinity for spectrin and for cytoplasmic domains of transmembrane transporters and channels promoting the link between spectrin and the plasma membrane [74]. Besides that, spectrin association with actin filaments in the cytoskeleton can be enhanced by other proteins, such as adducin [75]. Adducin, an actin filament binding protein localized in the plasma membrane of several tissues, is the key to the assembly of actin-spectrin complexes helping, also, in the maintenance of axonal actin rings [53, 75].

## 2.1 Characteristics and functions

Adducin comprises a family of proteins present in the vertebrate nervous system at high levels [76] specially in the growth cone and in pre-synaptic terminals of the axon [75]. It was originally purified in erythrocytes based on calmodulin binding activity which gave rise to the first name, Calmodulin Binding Protein [77, 78]. Now, it is known to be expressed in every tissue.

This protein, in mammalian cells, is encoded by three related genes: Add1, Add2 and Add3, which results in three isoforms: alpha ( $\alpha$ ), beta ( $\beta$ ) and gamma ( $\gamma$ ), and polypeptides with 726, 713 and 674 amino acids, respectively [79, 80]. The alpha and gamma isoforms (with 103 kDa and 84 kDa, respectively) are ubiquitously expressed, while the beta isoform (with 97 kDa) is more abundant in erythrocytes and brain [77, 79-82]. All three adducin proteins contain an N-terminal globular head domain, a neck domain and a C-terminal MARCKS (myristoylated alanine rich C-kinase substrate) protease-sensitive tail domain [79, 80, 83, 84]. This tail domain seems to be important in protein-protein interactions providing the specific site for spectrin and actin connection, although an oligomerization is required by adducin neck domain in order for this link to occur [75, 85]. So, the MARCKS domain is required but not sufficient for both adducin activities to be performed [86] (figure 11).

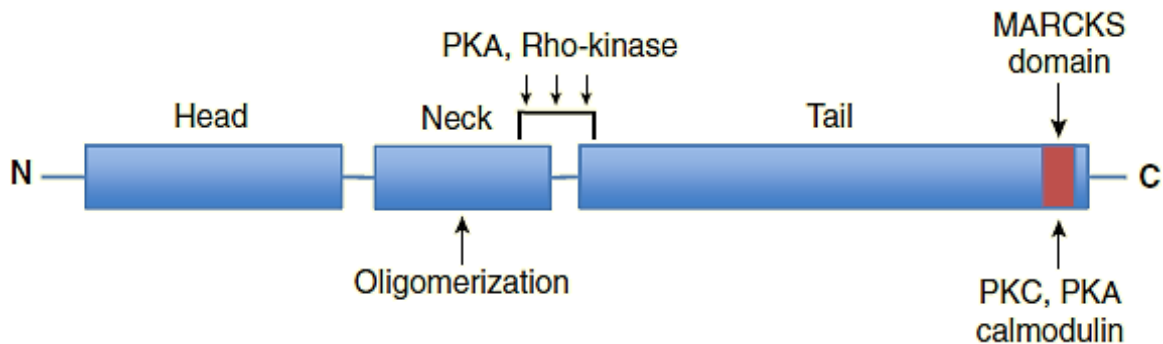


**Figure 11 – Schematic representation of adducin organization.** Adducin is composed by a globular head, a neck domain required for oligomerization and a C-terminal MARCKS tail domain important to protein-protein interaction. Adducin has several phosphorylated sites represented with arrows in the figure. Taken from [86].

Adducin is organized in heterotetramers of heterodimers through the interaction between its N-terminal globular head domain and the C-terminal tail MARCKS domain [75, 84], which comprises  $\alpha/\beta$  subunits and  $\alpha/\gamma$  subunits [77, 79, 84]. In the absence of the  $\alpha$  subunit, both  $\beta$  and  $\gamma$  isoforms are also absent despite normal mRNA expression levels [87]. In the absence of the  $\alpha$  isoform, the stability of the other two isoforms is severely compromised resulting in no adducin complex formation [87], which means that  $\alpha$ -adducin KO mice have an almost complete absence of adducin.

Adducin is a substrate for several protein kinases [75] and its activity is regulated by phosphorylation by protein kinase C (PKC), resulting in the inhibition of both actin-capping and spectrin-recruiting activities [88-90] and a decrease in actin and spectrin interaction. Ser726 of adducin is the major phosphorylation site for PKC, more specific to PKC  $\delta$  [91], but Ser662 and Ser716 can also be phosphorylation sites [89]. Adducin can also be phosphorylated by cyclic AMP (cAMP)-dependent protein kinase A (PKA) resulting in repression of both adducin activities (discussed below) [77, 78]. The phosphorylated form of adducin is mainly found in dendritic spines of neurons and it is believed that this phosphorylation is a response to external signals through changes in cell morphology and cytoskeleton organization [88].

A well studied adducin related protein is *hu-li tai shao* (hts), the adducin homolog in *Drosophila* [92-96]. Hts/Adducin was discovered in fusomes and ring canals being identified as an essential component for a normal oogenesis in flies and also required for the formation of the actin-spectrin structure [93, 97]. *Drosophila* adducin encodes four isoforms and one of those isoforms, known as Hts-M, has also a highly conserved MARCKS domain necessary for actin binding [95, 96].

Adducin was the first example of an actin capping protein that can recruit other proteins like spectrin to actin filament growing ends promoting the stability of actin subunits in the cellular cytoskeleton [75, 76].

## **2.2 Adducin and actin dynamics**

An efficient control of actin filaments in the cytoskeleton is crucial to neurons and this control of actin growth can be achieved by the action of ABPs, by capping the fast growing ends (barbed/plus ends) or capping the slower ones (pointed/minus ends) [98]. There are some important ABPs such as spectrin, protein 4.1, tropomyosin, tropomodulin, protein 4.9 and adducin [75, 85, 98] that can efficiently regulate actin. In fact, adducin,

localized at spectrin-actin junctions [99], is crucial for the assembly of spectrin-actin networks [72, 100].

Capping proteins like adducin have a high affinity for the barbed ends of actin and depletion or dysfunction of these proteins promotes an increase in actin filament assembly. Since adducin is responsible for capping the actin ends, this ABP can control actin polymerization, blocking the elongation and depolymerization of actin [98]. Therefore, adducin can inhibit the incorporation of new monomers of actin, preventing the addition or loss of actin subunits. This allows a more stable state of actin [75] (figure 12).

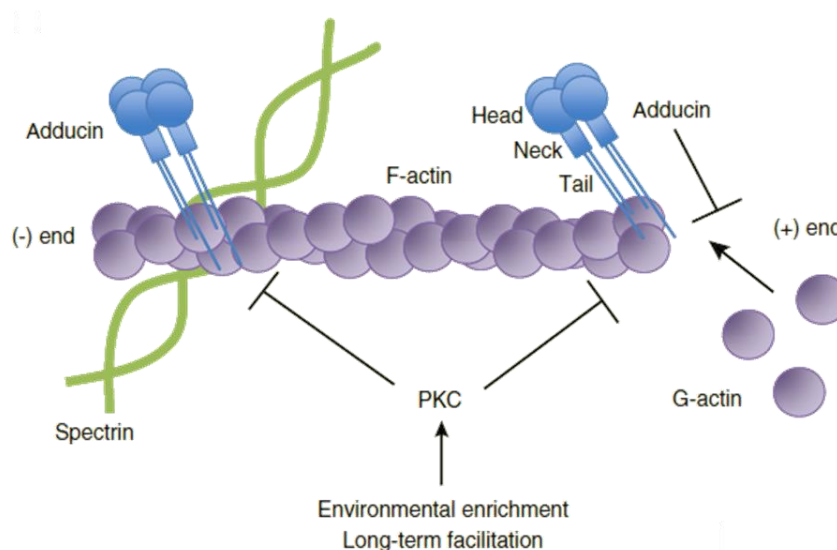


**Figure 12 – Adducin organization and regulation.** Adducin can cap the fast-growing ends of actin preventing the addition or loss of actin subunits. The phosphorylation of adducin by PKC promotes the actin-spectrin network dissociation resulting in inhibition of actin-capping activity. This allows a more dynamic state of actin. Taken from [86].

Besides its capping activity, adducin is also able to promote the spectrin-actin interaction, recruiting spectrin to actin filament ends playing a critical role in the assembly of new spectrin molecules to the ring complexes [76, 84]. This protein can bind to the spectrin-actin complexes with high affinity but also bind to each of the proteins alone with a lower affinity [71].

It is known that adducin phosphorylation leads to a decrease in adducin action which results in no actin-capping or spectrin-recruiting activities [77, 78, 88] leading to

actin filament growth and polymerization and, consequently, an increase in actin instability and a more dynamic state of the cytoskeleton [86]

As such, regulation of adducin activity is essential for, either stability of the cytoskeleton or morphology of synapses [86].

### **2.3 Adducin and actin rings**

As detailed above, adducin is a protein with the dual function of capping barbed actin ends and crosslinking actin-spectrin networks in the rings [53]. As described before, this ring pattern starts to be formed at early stages of development. At DIV2, when the break of symmetry originates the axon and dendrites, the spectrin rings are already present being propagated along the axon towards its distal end. Adducin only starts to appear in the actin rings at DIV6 becoming clearly distributed in this structure at DIV7 [55]. So, initially, with the absence of adducin, there is a more unstable state of actin. With cell maturation, the actin rings become more stable, probably due to the presence of adducin and of its capping activity. In this way, loss of adducin in neurons may contribute to a decreased actin stability at early developmental stages [55].

### **2.4 Preliminary results: $\alpha$ -adducin KO mice develop progressive axon enlargement and degeneration**

Knockout models (KO) of actin regulating proteins arose as relevant models to study and comprehend which regulators of the actin cytoskeleton are physiologically important. In this work we used  $\alpha$ -adducin KO mice as a model to study the importance of this protein in the axon cytoskeleton. To understand the relevance of adducin's loss in neuron biology, we analyzed the central and peripheral nervous system of  $\alpha$ -adducin KO mice. In the central nervous system, the absence of  $\alpha$ -adducin led to axon loss in both the optic nerve (figure 13A and 13B) and the spinal cord (figure 13D and 13E). In the optic nerve, axon loss was progressive since normal axon density was observed at postnatal day 20 (P20), but by P100  $\alpha$ -adducin KO optic nerves had a 40% reduction of axon density (WT: 731044 axons/mm<sup>2</sup>  $\pm$ 22718;  $\alpha$ -adducin KO: 444215 axons/mm<sup>2</sup>  $\pm$ 63918;  $p < 0.01$ ) (Figure 13B). At this age, we also observed severe atrophy (figure 13C) with a 33% decreased optic nerve area in mutant nerves (WT: 0.088mm<sup>2</sup>  $\pm$ 0.002;  $\alpha$ -adducin KO:

0.058mm<sup>2</sup> ±0.005; p<0.001). Overall, the decreased axon density and nerve crosssectional area resulted in an estimated loss of 60% of the total number of axons in  $\alpha$ -adducin KO optic nerves. A decreased axon density was also visible in  $\alpha$ -adducin KO spinal cords. Analysis of the corticospinal tract (CST) revealed a 25% decreased axonal density in the absence of  $\alpha$ -adducin (WT: 462197 axons/mm<sup>2</sup> ±35667;  $\alpha$ -adducin KO: 305513 axons/mm<sup>2</sup> ±13447; p<0.05) (figures 13D and 13E). In the peripheral nervous system, we also observed a decreased density of myelinated axons in sciatic nerves from  $\alpha$ -adducin KO mice (data not shown). Combined, these results support previous analyses in the PNS [87], and highlight that loss of adducin has a major impact in central and peripheral nervous system axons. Interestingly, progressive axonal enlargement preceded axon loss in  $\alpha$ -adducin KO mice. The distribution of axons of different diameters was normal in the P20 optic nerve, but by P60 an increase in high diameter (> 2  $\mu$ m) axons was observed and was exacerbated at P100 where an overall decrease in small diameter axons was accompanied by an increase in large diameter axons (figures 13F, 13G and 13H). Interestingly, myelin thickness as determined by the g-ratio was similar in the optic nerve of P100 WT and  $\alpha$ -adducin KO mice (data not shown) suggesting that enlarged axons are normally myelinated. Abnormally large axons were also found in the spinal cord (figure 13D, asterisks) and sciatic nerve (figure 13I, asterisks).

In summary, our results show that in the absence of adducin, there is an enlargement of axon diameter and axonal loss in both the CNS and PNS.

In this Thesis we evaluated some of the causes that may underlie this phenotype.



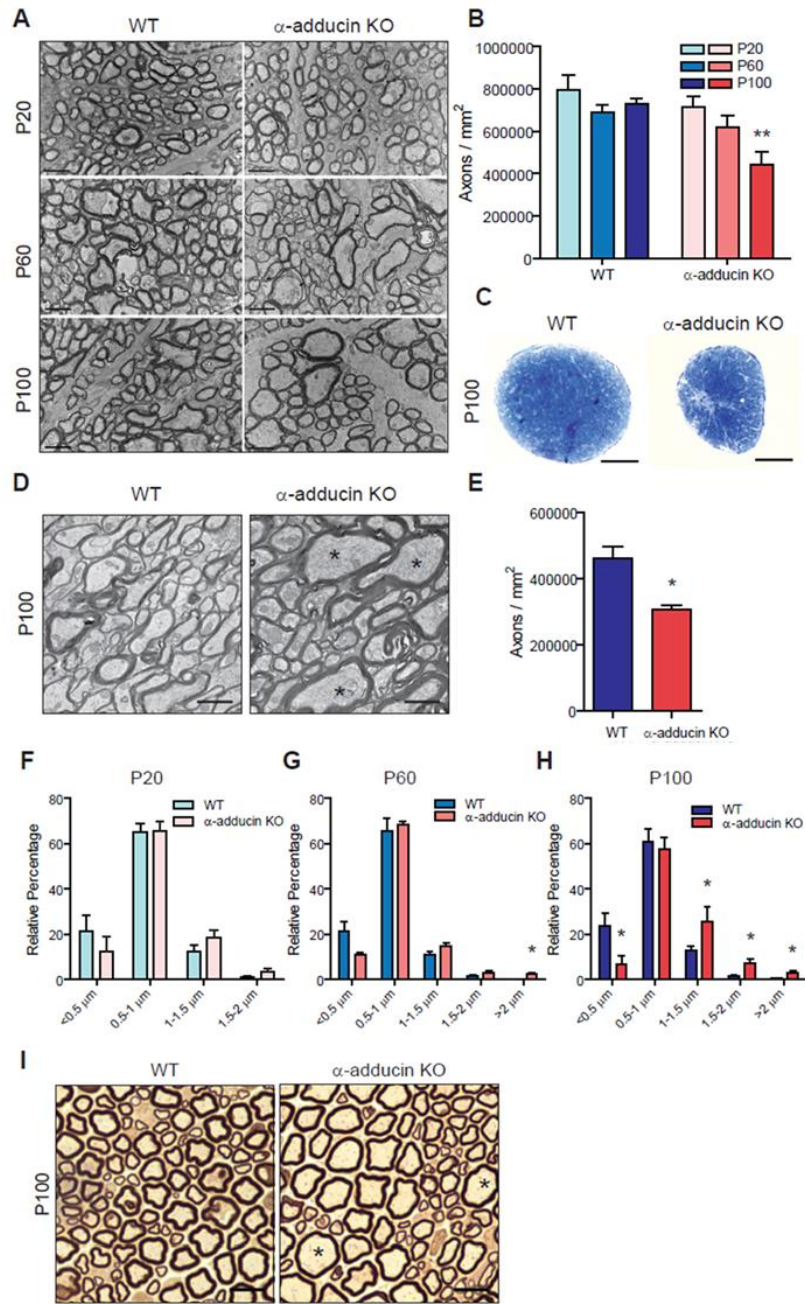


**Figure 13 –  $\alpha$ -adducin KO mice show progressive axon enlargement and axonopathy.** (A) Representative 12000x microphotographs of ultra-thin sections of optic nerves from WT and  $\alpha$ -adducin KO mice at P20, P60 and P100; Scale bar: 2  $\mu$ m. (B) Axon density in the optic nerve of WT (P20 n=4; P60 n=5; P100 n=5) and  $\alpha$ -adducin KO mice (P20 n=4; P60 n=5; P100 n=4) at P20, P60 and P100. (C) Representative semi-thin cross sections of WT and  $\alpha$ -adducin KO optic nerves stained with toluidine blue; Scale bar: 100  $\mu$ m. (D) Representative 6000x microphotographs of ultra-thin sections of WT and  $\alpha$ -adducin KO corticospinal tracts; asterisks highlight axons with enlarged diameter; Scale bar: 1  $\mu$ m. (E) Axon density in the corticospinal tract of WT (n=4) and  $\alpha$ -adducin KO mice (n=4) at P100. (F-G) Axon distribution according to diameter in P20 (F), P60 (G) and P100 (H) WT (P20 n=5; P60 n=4; P100 n=6) and  $\alpha$ -adducin KO (P20 n=4; P60 n=4; P100 n=5) optic nerves. (I) Representative semi-thin sections of WT and  $\alpha$ -adducin KO sciatic nerves; asterisks highlight axons with enlarged diameter; Scale bar: 10  $\mu$ m. Graphs show mean  $\pm$  SEM; p-value \* $<$ 0.05, \*\* $<$ 0.01.

## Objectives

In this work we propose to determine the importance of adducin in the axonal cytoskeleton and, more specifically, in axonal transport, as defects in axonal transport have been related to axon enlargement. We also aim at comprehending the importance of adducin in another important aspect of neuron biology that is the plasticity of the axon initial segment that requires actin dynamics.

Specifically, the aims of this work were:

- A. Understand the effect of adducin in axonal transport by *in vivo* analysis and through live imaging of organelles and vesicles in *in vitro* cultures.
- B. Comprehend the influence of adducin in the plasticity of the axon initial segment.

In sum, with this project we will contribute to the understanding of how a specific actin-binding protein, adducin, participates in neuronal biology.

# Materials and Methods

## Animals

Mice were handled according to European Union and National legislation. The protocols here described have been approved by the IBMC Ethical Committee and by the Portuguese Veterinarian Board. Mice were bred in the animal house facility of the IBMC with *ad libitum* access to water and rodent food, and were kept on a 12 hour light and dark cycle. The  $\alpha$ -adducin KO mice and WT littermates were obtained from heterozygous breeding pairs and genotyped by IBMC CCGen facility, as described [87]. Mice were sacrificed by using over-dose anesthesia followed by decapitation.

## Primary neuron cultures

### Dorsal root ganglia neuron cultures

DRG were collected from 30 days old  $\alpha$ -adducin KO and WT mice and digested with 0.125% collagenase-IV-S (Sigma, C1189) for 90 minutes at 37°C with 5% CO<sub>2</sub>. After enzyme treatment, washing and centrifugation for 20 seconds at 300 rpm, using fire-polished Pasteur pipettes, a single cell solution was obtained by dissociation. The cell suspension was centrifuged into a 15% BSA (NZYTech) gradient for 10 min at 1000 rpm. The obtained pellet was resuspended in DMEM/F12 medium (Sigma, D8437) supplemented with 1% penicillin-streptomycin (Gibco), 2× B27 (Gibco), 2mM L-glutamine (Gibco), 50 ng/ml NGF (Millipore, 01-125) and plated at 3750 cells/well in 8-well  $\mu$ -dishes coated with 20 $\mu$ g/mL poly-L-lysine (Sigma, P2636) and 5 $\mu$ g/mL laminin (Sigma, L2020). The cells were maintained at 37°C with 5% CO<sub>2</sub> for 2 days.

### Hippocampal neuron cultures

Hippocampi were dissected from E17.5 embryos and the animals' tails were used for genotyping. The hippocampus of each individual pup was digested with 0.06% porcine trypsin solution (Sigma, T4799) in HBSS for 15 minutes at 37°C with 5% CO<sub>2</sub>. After enzyme treatment and washing, the hippocampi were resuspended in Neurobasal

medium (Invitrogen) and a single-cell suspension was obtained by passing the solution up and down in a micropipette and through a 70  $\mu\text{m}$  cell strainer. The single-cell suspension was resuspended in Neurobasal medium (Invitrogen) supplemented with 1% penicillin-streptomycin (Gibco), 2 $\times$  B27 (Gibco) and 2 mM L-glutamine (Gibco), and plated either at 16000 cells/well in 24-well plates containing pre-coated glass cover slips treated with 20  $\mu\text{g}/\text{mL}$  poly-L-lysine (Sigma, P2636) - for axon initial segment analysis, or 12200 cells/well in 8-well  $\mu$ -dishes coated with 20  $\mu\text{g}/\text{mL}$  poly-L-lysine - for axonal transport assays. For axon initial segment analysis, the cells were maintained at 37°C with 5% CO<sub>2</sub> for 10 days and for axonal transport assays, they were maintained for 4 days.

## **Immunofluorescence**

### **Adducin immunofluorescence**

DIV16 hippocampal neurons were treated with 0.1% Triton-X, blocked and incubated with the primary antibodies rabbit anti-adducin, 1:200 (Abcam, ab51130) and mouse anti  $\beta$ III-tubulin, 1:5000 (Promega, G7121). Secondary antibodies used were donkey-anti-mouse Alexa Fluor 488 and donkey-anti rabbit Alexa Fluor 568, both diluted 1:1000 (Invitrogen, A-21202 and A10042 respectively). Coverslips were mounted in fluoroshield (Sigma). Images were acquired in a Leica DMI 6000B inverted microscope at 40x.

## ***In vivo* axonal transport assay**

### **Intravitreal injection of cholera toxin B**

*In vivo* transport assays were performed in 6 months old WT (n=4) and  $\alpha$ -adducin KO (n=4) mice. Mice were anesthetized with ketamine (75 mg/kg) and medetomidine (1 mg/kg) and analgesia with buprenorphine (0.08 mg/kg) was done prior to the surgical procedure. Eyes were wet with local optic anesthetic (1 drop per eye). Injection was performed intravitreally in a 45° angle with a 30-33 gauge needle syringe with 2  $\mu\text{l}$  of the 0.1% cholera toxin subunit  $\beta$  conjugated with Alexa Fluor 568 (List Biological Laboratories) with a rate of 1  $\mu\text{l}$  per 15 seconds, at most.

## **Optic nerve analysis**

Twelve hours after injection animals were sacrificed and perfusion with 4% PFA was performed. Optic nerves were post-fixed 1 hour in 4% PFA and then incubated overnight in a 30% sucrose (in PBS) solution. The equilibrated nerves were then sectioned at 14  $\mu\text{m}$ . Sections were mounted in fluoroshield (Sigma) and Alexa Fluor 568 fluorescence was acquired. Analysis was performed in ImageJ software, by drawing a line 250  $\mu\text{m}$  wide from the tip to the end of the optic nerve segment. Analysis was performed in the segment going from the initial region of the optic nerve (0  $\mu\text{m}$ ) up to a distance of 2400  $\mu\text{m}$ . Intensity of fluorescence was plotted by the distance averaging it every 50  $\mu\text{m}$  and then normalizing it to 100% to the maximum fluorescence level.

## ***In vitro* axonal transport assay**

### **Live imaging of axonal transport**

Hippocampal and DRG neuron cultures were performed as detailed above. For the live imaging of axonal transport, DIV4 (DIV5 for synaptophysin) hippocampal neurons (a timepoint at which their polarized morphology allows the clear identification of the axon as the longest neurite) or DIV2 (DIV3 for synaptophysin) DRG neurons were used. Cells were incubated for 45 minutes with 100nM of either LysoTracker (Invitrogen), Mitotracker (Invitrogen) or Synaptophysin-GFP (Cell Light) in complete DMEM:F12 medium. After that, for Mitotracker and LysoTracker, cells were washed with DMEM:F12 without phenol red and incubated for 1 hour with complete plating medium without phenol red at 37°C till live imaging. For synaptophysin, cells were maintained in complete medium overnight. The next day, cells were washed with DMEM:F12 without phenol red and incubated with complete plating medium without phenol red at 37°C for 1 hour.

### **Analysis of axonal transport and quantification**

Transport of axonal mitochondria, lysosomes and synaptic vesicles was analyzed in a Leica SP5II confocal microscope (Leica Microsystems) with acquisition at 0.8 Hz for 2 min. Photomicrographs were taken for 2 min with 1 sec frame intervals with 4 Z-stacks per frame. The analysis of axonal transport (velocity and dynamic) was done using the Fiji software, through the measurement of the speed of the vesicles or organelles in both

directions of movement. The vesicles that were not moving were also counted. For quantification, only vesicles and organelles moving for 10 consecutive frames were considered. For the analysis of velocity, at least 70 vesicles or organelles in DRG neurons (from at least 13 different cells) were measured, and at least 85 were analysed in hippocampal neurons (from at least 12 different cells).

### **Axon initial segment assay**

Hippocampal neurons were maintained at 37°C with 5% CO<sub>2</sub> for 10 days and then incubated with 15mM of either NaCl (control) or KCl (depolarizing agent) for 48 hours.

### **Immunofluorescence**

At DIV12, cells were fixed with warm 2% PFA. Cells were treated with 0.1% Triton-X/PBS and with 0.1M NH<sub>4</sub>Cl/PBS. Hippocampal neurons were incubated for 1 hour at RT with 5% blocking buffer (fetal bovine serum [FBS]), in PBS. Primary antibodies, mouse anti-ankyrinG (1:100; Calbiochem, NB20) and rabbit anti-βIII tubulin (1:1000; Cell Signaling Technology, 5142). Antibodies were diluted in blocking buffer and incubated overnight at 4°C. After washing with PBS, secondary antibodies, donkey anti-mouse Alexa Fluor® 488 and donkey anti-rabbit Alexa Fluor® 568 (1:1000; Invitrogen, A-21202 and A10042 respectively) were diluted in blocking buffer and incubated for 1 hour at RT. Then, the coverslips were washed and mounted with fluoroschild (Sigma, F6057) containing DAPI (Vector Labs). Cells were analysed by epifluorescence on a Zeiss Axio Imager Z1 microscope equipped with an AxioCam MR3.0 camera and Axiovision 4.7 software, at 63x magnification.

### **Axon initial segment analysis**

The axon initial segments were analyzed using FIJI software. The ankyrinG fluorescence staining profile was plotted from the soma membrane throughout the axon, and the delimitation of the axon initial segment size was done by measuring the segment with at least 33% of the maximum fluorescence (100% being the point of maximum

intensity, and 0% being the point of lower intensity). The start and end points were the proximal and distal drop in fluorescence intensity, respectively.

## Western blotting

Protein lysates from brain extracts from  $\alpha$ -adducin KO and WT P30 mice were prepared by sonication in PBS containing 0.3% Triton X-100, protease inhibitor cocktail (cOmplete, Mini; Roche), and 2 mM orthovanadate. Total protein of each sample was determined using the Bio-Rad DC Kit.

For analyses under denaturing conditions, 10% SDS-PAGE gels or Criterion XT 3-8% gradient gels (Bio-rad), were run with 25  $\mu$ g of brain, spinal cord or optic nerve extracts from wt (n=3) and  $\alpha$ -adducin KO (n=3) P30 mice. For analyses of post-translational modifications of tubulin and molecular motors, 10% SDS-PAGE gels were run with 5  $\mu$ g of brain extracts from WT (n=9) and  $\alpha$ -adducin KO (n=5) P30 mice. Gels were transferred to nitrocellulose membranes for 2 hours using a semi-dry system. For analyses under native conditions, 4% PAGE gels were used with 50  $\mu$ g of brain extracts from wt (n=3) and  $\alpha$ -adducin KO P30 mice (n=3). Native gels were run and transferred to a PVDF membrane for 2 hours using a semi-dry system.

Membranes were washed in Tris buffered saline (TBS) with 0.1% Tween-20, blocked in 5% non-fat dried milk (Sigma-Aldrich) in TBS with 0.1% Tween-20 for 1 hour at room temperature, and incubated with primary antibodies (in 5% BSA in TBS with 0.1% Tween-20) overnight at 4°C.

The following primary antibodies were used: rabbit anti-adducin (1:1000, Abcam), mouse anti- $\beta$ -actin (1:5000, Sigma), mouse anti-capping protein  $\alpha$ 1/2 (1:50, Developmental Studies Hybridoma Bank), mouse anti-capping protein  $\beta$ 2 (1:150, BD Developmental Studies Hybridoma Bank), mouse anti-acetylated tubulin (1:40000, Sigma), mouse anti- $\alpha$ -tubulin (1:10000, Sigma), rat anti-tyrosinated tubulin (1:4000, AbD Serotec), rabbit anti-de-tyrosinated tubulin (1:4000, Millipore), mouse anti-cytoplasmic dynein (1:250, Millipore) and mouse anti-kinesin heavy chain (1:1000, Millipore).

Membranes were washed and incubated with secondary antibodies in 5% non-fat dried milk in TBS for 1 hour, at room temperature. The secondary antibodies used were: donkey anti-mouse IgG, donkey anti-rat IgG or donkey anti-rabbit IgG conjugated with HRP, (1:5000, Jackson). Membranes were then incubated for 5 minutes at room temperature with Luminata Forte Western HRP (Millipore) and chemiluminescence was

analyzed by exposure to Amersham Hyperfilm ECL (GE healthcare). Films were scanned on a Molecular Imager GS800, and Quantity One (Bio-Rad) was used for quantifications.

### **Statistical analysis**

Results were expressed as the mean  $\pm$  SEM, and data were analyzed with Prism software (GraphPad Software). Statistical significance was determined by Student's t test.



# Results

## I. $\alpha$ -adducin KO mice lack functional adducin tetramers.

Functional adducin consists of a tetrameric complex of two heterodimers where the  $\alpha$  monomer is essential. We started by analyzing whether in the nervous system, similarly to what happens in erythrocytes [87], the absence of  $\alpha$ -adducin results in decreased levels of  $\beta$ - and  $\gamma$ -adducin. In fact, the nervous tissue from  $\alpha$ -adducin KO mice had severely decreased levels of  $\beta$ - and  $\gamma$ -adducin (figure 14A), similarly to what is observed in erythrocytes from  $\alpha$ -adducin KO mice [87]. Consistently, in  $\alpha$ -adducin KO mouse brains no dimer/tetramer formation was visualized by western blot after native PAGE (figure 14B). In the absence of  $\alpha$ -adducin, capping protein (EcapZ) levels were similar to those found in WT animals (figure 14C). Immunofluorescence of hippocampal neurons further confirmed the absence of adducin in  $\alpha$ -adducin KO neurons (figure 14D). After having confirmed that  $\alpha$ -adducin KO mice lack functional adducin, we examined this model to further uncover adducin's function in the development and homeostasis of the nervous system.

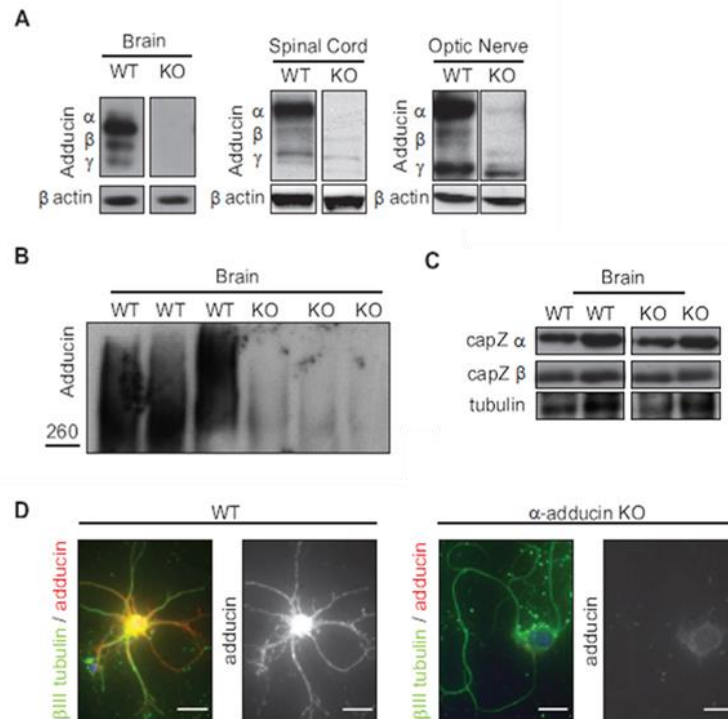


**Figure 14 –  $\alpha$ -adducin KO mice have severely decreased levels of  $\beta$ - and  $\gamma$ -adducin and lack functional adducin tetramers.** (A) Western blot analysis of brain, spinal cord and optic nerve of WT and  $\alpha$ -adducin KO mice using a pan-specific antibody that recognizes the in  $\alpha$ -,  $\beta$ - and  $\gamma$ -adducin forms [53]. (B) Anti-adducin

western blot analysis of brain extracts of WT and  $\alpha$ -adducin KO brain extracts run on native gels. The 260 kDa standard is indicated (note that under reducing conditions the observed MW of an adducin dimer is of approximately 210-260 kDa [77]). (C) Western blot analysis of capping protein (ECapZ) in brain extracts of WT and  $\alpha$ -adducin KO mice. (D) Anti-adducin immunofluorescence in E16 hippocampal neurons isolated from WT and  $\alpha$ -adducin KO mice. Left panels: DAPI (blue),  $\beta$ III-tubulin (green) and pan-adducin (red); right panels: pan-adducin (white). Scale bar: 10  $\mu$ m

## **II. The lack of adducin does not produce a significant effect in the transport of cholera toxin through the optic nerve.**

As mentioned in the Introduction,  $\alpha$ -adducin KO mice display axon degeneration and enlargement. Since defects in axonal transport have been related with axonal degeneration and enlargement [63, 101-104], understanding the role of adducin in axonal transport was necessary. For that, we started by analyzing the effect of the lack of adducin in axonal transport by performing an *in vivo* assay consisting of an intravitreal injection of cholera toxin subunit  $\beta$  conjugated with a fluorescent label in the eye of 6 months old WT and  $\alpha$ -adducin KO mice.

In the past years, cholera toxin subunit  $\beta$  (CTB) has been widely used in axonal transport assays [105-116] due to its high ability to move in both directions of the axon, retrogradely and anterogradely, from the site of injection, labelling the entire neuron, including processes and terminals of the mammalian nervous system such as the visual pathway [105]. CTB binds to gangliosides on the surfaces of mammalian cells and many fluorescent molecules have been attached to CTB such as Alexa Fluor creating an efficient neuroanatomical tracer [106]. Given the phenotype of  $\alpha$ -adducin KO mice we hypothesized that maybe these animals might present some defect in axonal transport, resulting in a decreased CTB transport along the axon. After CTB injection, mice were sacrificed and the optic nerves analyzed. The intensity of fluorescence was evaluated along the animals' optic nerves, by quantifying the fluorescence from the tip to the end of the optic nerve axons. However, as shown in figure 15, there were no significant changes in the fluorescence's intensity between WT and  $\alpha$ -adducin KO optic nerves.

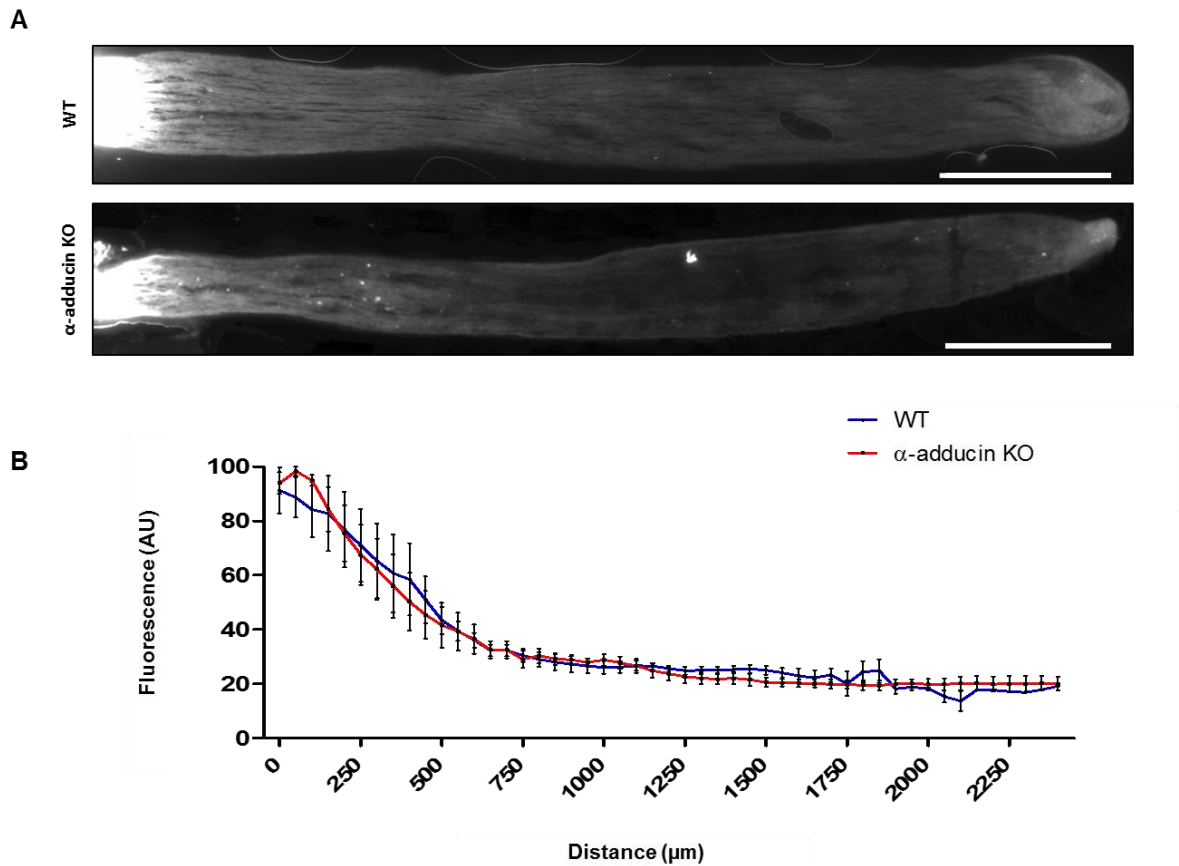


**Figure 15 – In vivo axonal transport analysis after CTB injection in the eye of 6 months old WT and  $\alpha$ -adducin KO mice.** (A) Representative longitudinal images of the optic nerve of WT (n=4) and  $\alpha$ -adducin KO (n=4) mice; scale bar: 1  $\mu\text{m}$ . (B) Intensity of fluorescence along the optic nerve. The intensity of fluorescence was normalized (100% - maximum fluorescence level). The fluorescence measurements were performed from the beginning of the optic nerve (0  $\mu\text{m}$ ) to the distance of 2400  $\mu\text{m}$ .

Therefore, since the analysis of the *in vivo* transport of cholera toxin assay did not provide any significant effect of the lack of adducin in axonal transport, we followed by using alternative methods that have a higher sensitivity to detect defects in the transport mechanisms and machinery.

### III. The lack of adducin generates an impairment of the axonal transport of mitochondria and lysosomes.

With the aim of further unraveling the impact of adducin in axonal transport, we performed *in vitro* analyzes of the movement of organelles (mitochondria and lysosomes) and synaptic vesicles in cultures of dorsal root ganglion (DRG) neurons and embryonic hippocampal neurons of WT and  $\alpha$ -adducin KO mice.

In DRG neurons a significant decrease in the speed of axonal transport of mitochondria both in the anterograde and retrograde directions was observed (figure 16A), whereas in lysosomes, a defect was only apparent in the retrograde direction (figure 16B). Interestingly, in the case of synaptic vesicles, no statistical differences in the speed of axonal transport were detected between WT and  $\alpha$ -adducin KO cells (figure 16C).

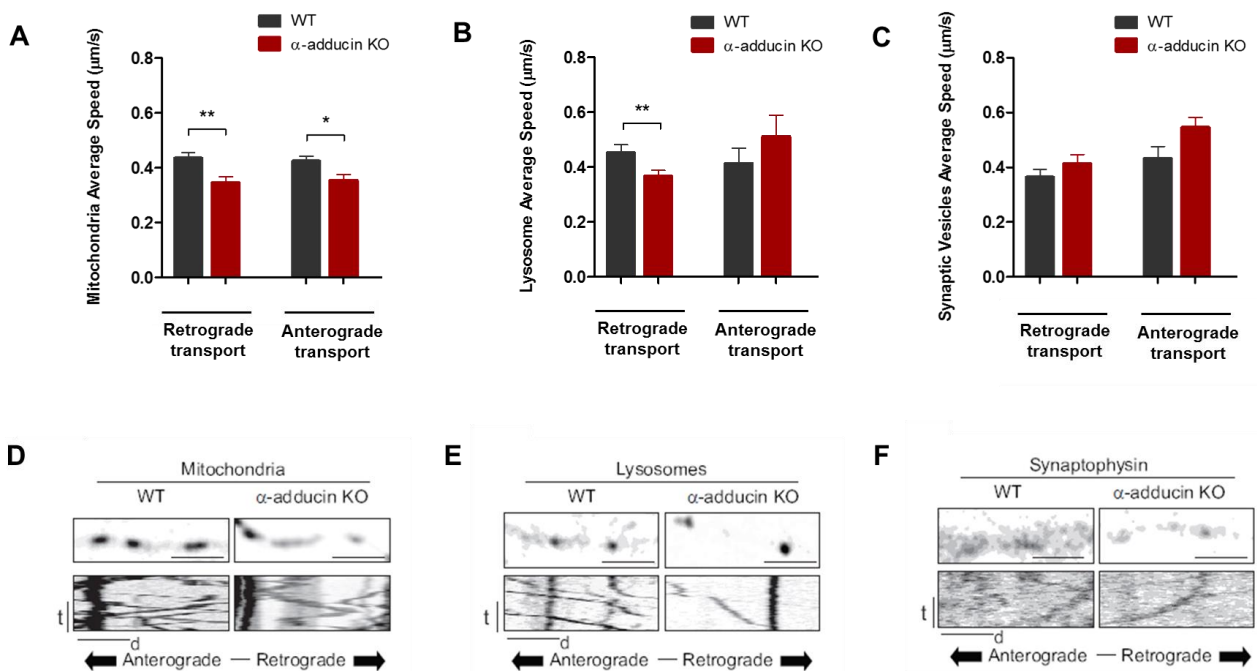


**Figure 16 – Analysis of the axonal transport speed of WT and  $\alpha$ -adducin KO DRG neurons.** (A-C) Quantification of the axonal transport speed of (A) mitochondria, (B) lysosomes and (C) synaptic vesicles. Graphs show mean  $\pm$  SEM; p-value  $<0.05$ ,  $<0.01$ . (D-F) Upper- still images at t=0 and lower- kymographs, of (D) mitochondria, (E) lysosomes and (F) synaptophysin. Scale bar: time (t): 100 seconds; distance (d): 5  $\mu$ m

In embryonic hippocampal neurons, similar findings were obtained with both mitochondria (figure 17A) and lysosomes (figure 17B) presenting a decreased speed of axonal transport both in the anterograde and retrograde directions in  $\alpha$ -adducin KO cells and with synaptic vesicles having no apparent defects in the speed of axonal transport (figure 17C).

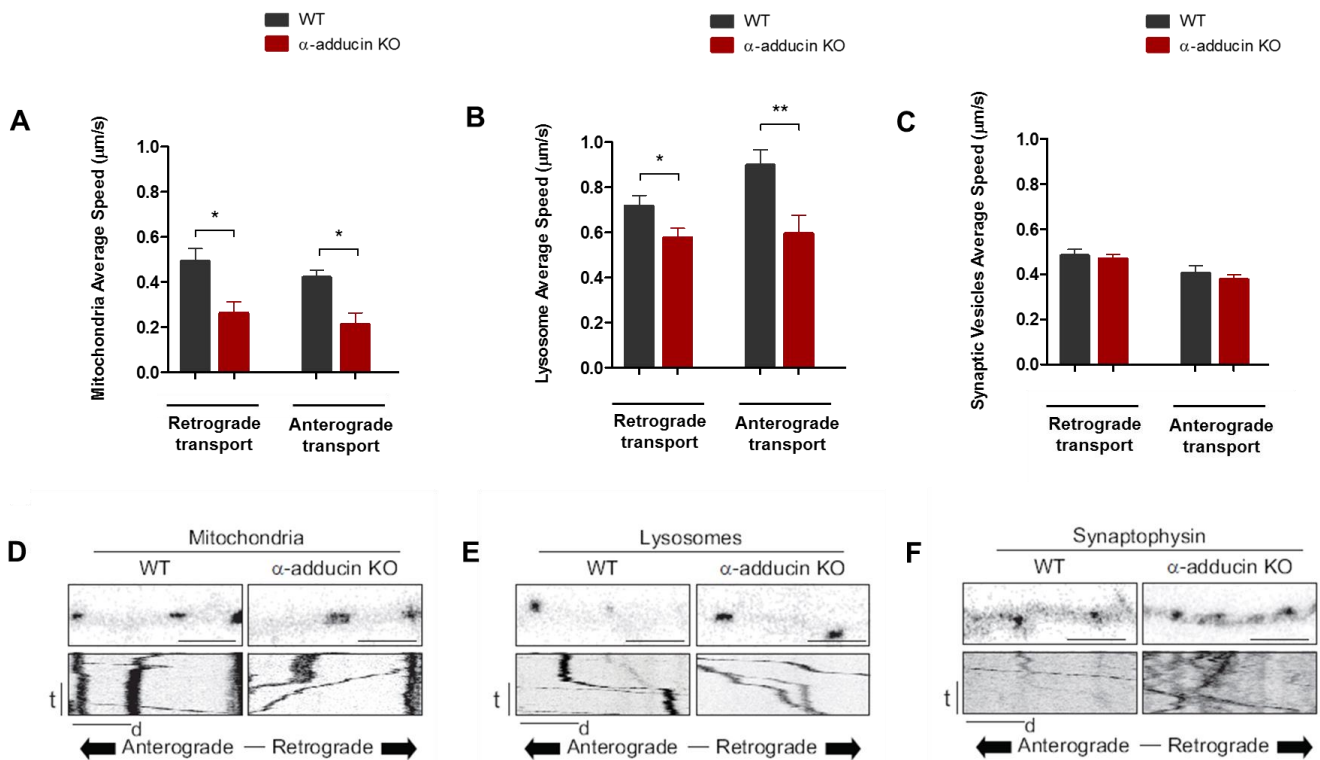


**Figure 17 – Analysis of the axonal transport speed of WT and  $\alpha$ -adducin KO embryonic hippocampal neurons.** (A-C) Quantification of the axonal transport speed of (A) mitochondria, (B) lysosomes and (C) synaptic vesicles. Graphs show mean  $\pm$  SEM; p-value  $<0.05$ ,  $**<0.01$ . (D-F) Upper- still images at t=0 and lower- kymographs, of (D) mitochondria, (E) lysosomes and (F) synaptophysin. Scale bar: time (t): 100 seconds; distance (d): 5  $\mu$ m

Besides measuring the speed of axonal transport of organelles and vesicles, we also quantified the dynamics of transport both in DRG and embryonic hippocampal neurons. For that, we determined the percentage of organelles and vesicles that were moving (or not), in each of the directions of movement.

In DRG neurons, whereas there was a decrease in the percentage of lysosomes moving in the anterograde direction (figure 18B), no major alterations were found in the percentage of moving vesicles in the case of mitochondria (figure 18A) and synaptic vesicles (figure 18C).

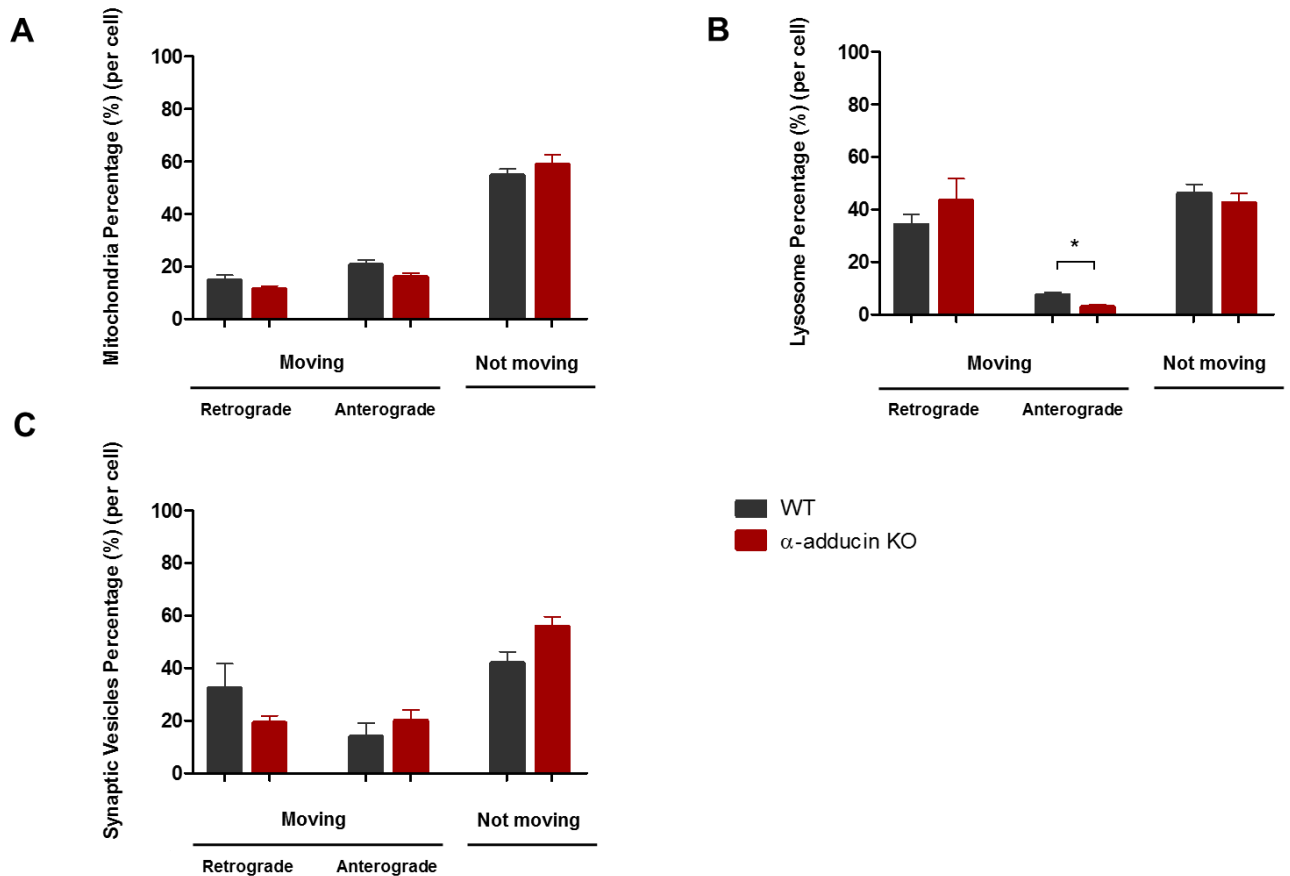


**Figure 18 – Analysis of the percentage of moving cargos in WT and  $\alpha$ -adducin KO DRG neurons.** Quantification of the percentage of moving (A) mitochondria, (B) lysosomes and (C) synaptic vesicles. Graphs show mean  $\pm$  SEM; p-value \* < 0.05.

Such as in DRG,  $\alpha$ -adducin KO embryonic hippocampal neurons had no significant differences in the percentage of moving mitochondria (figure 19A) and lysosomes (figure 19B) while the percentage of synaptic vesicles moving in retrograde direction is decreased (figure 19C).

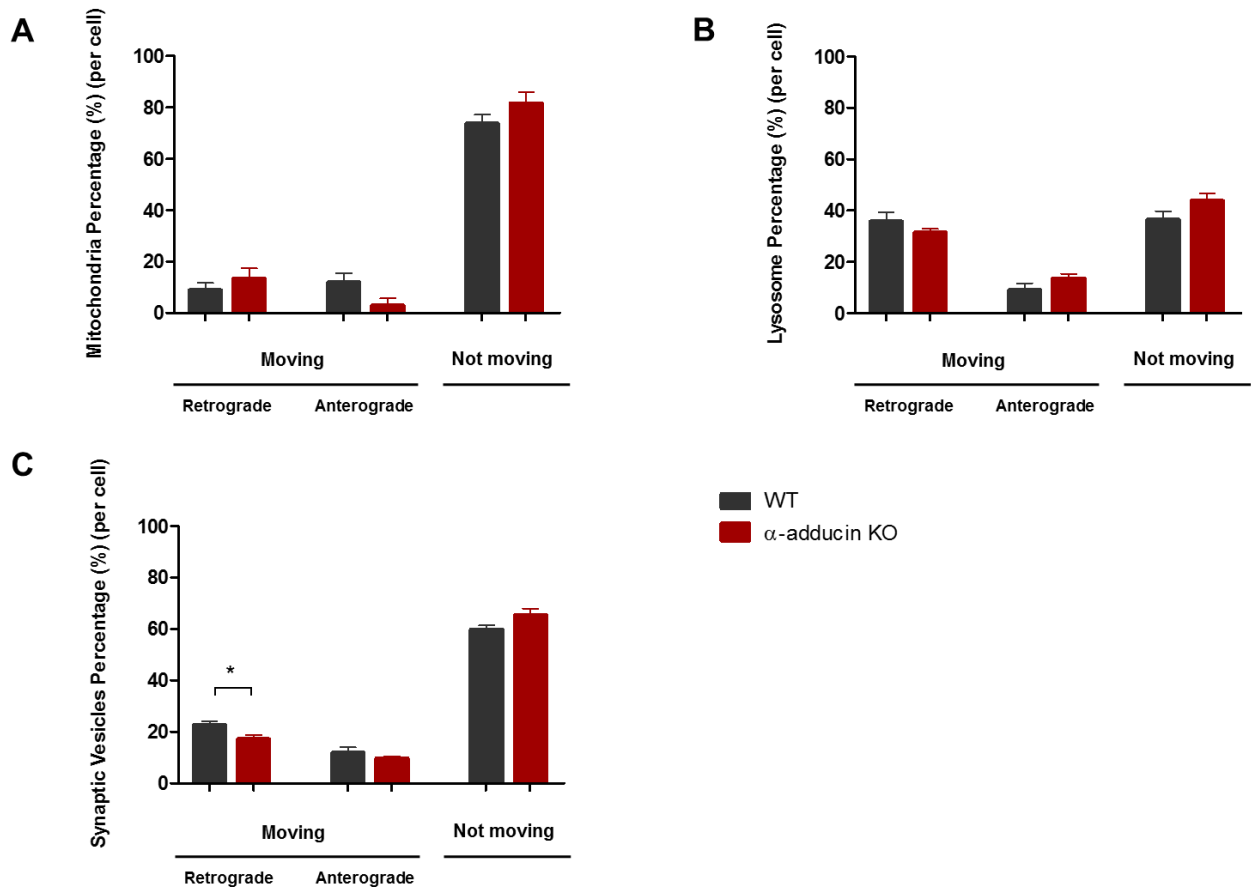


**Figure 19 – Analysis of the percentage of moving cargos in WT and  $\alpha$ -adducin KO embryonic hippocampal neurons.** Quantification of the percentage of moving (A) mitochondria, (B) lysosomes and (C) synaptic vesicles. Graphs show mean  $\pm$  SEM; p-value  $< 0.05$ .

In summary, our data supports that the lack of adducin has a strong effect in decreasing the speed of axonal transport of organelles although the percentage of moving cargos remains relatively unchanged.

#### IV. The absence of adducin results in decreased levels of tyrosinated tubulin and of molecular motors.

Given the important role of microtubules in axonal transport [117, 118], we asked whether alterations in the microtubule post-translational modifications (PTMs) interfere with transport. So, we analyzed if there were differences in the levels of acetylation, tyrosination and de-tyrosination of tubulin when comparing WT and  $\alpha$ -adducin KO neurons. High levels of acetylated tubulin and of de-tyrosinated tubulin are indicative of a more stable state cytoskeleton while tyrosinated tubulin appears to be increased if the cytoskeleton is more unstable and dynamic [118-120]. To explore this hypothesis, we performed western blot analysis of different tubulin modifications in brains from 30 days old WT and  $\alpha$ -adducin KO animals (figure 20A). No differences were found in the levels of acetylated and de-tyrosinated tubulin when comparing WT and  $\alpha$ -adducin KO brains (figure 20B and 20D) whereas the levels of tyrosinated tubulin were significantly decreased in  $\alpha$ -adducin KO mice (figure 20C), which suggests that in the absence of adducin the microtubule cytoskeleton is less dynamic.

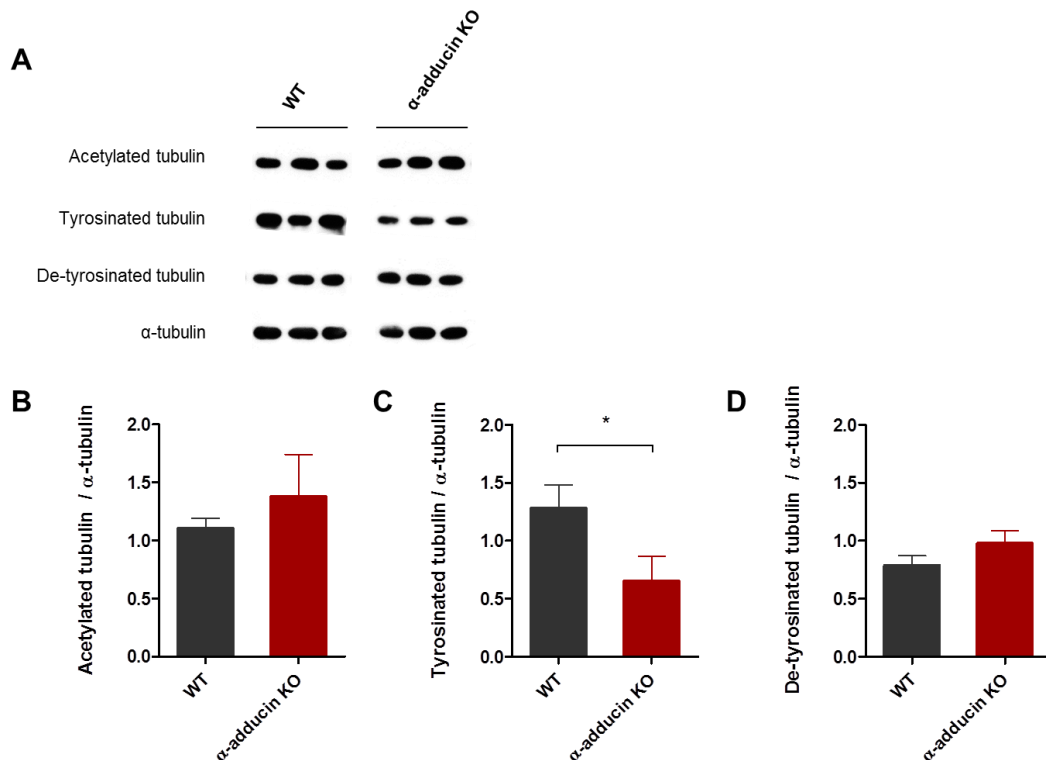


**Figure 20 – Analysis of the levels of post-translational modifications of tubulin in WT and  $\alpha$ -adducin KO mouse brains.** (A) Representative Western blot. (B-D) Quantification of the levels of (B) acetylated, (C) tyrosinated and (D) de-tyrosinated tubulin in brain tissue samples from  $\alpha$ -adducin KO and WT P30 mice. Graphs show mean  $\pm$  SEM; p-value  $<0.05$ .



Besides tubulin PTMs, axonal transport might be affected by a differential activity/availability of molecular motors i.e, dynein and kinesin that are the microtubule-dependent motors responsible for the retrograde and anterograde transport, respectively. To verify the levels of these two molecular motors in the cellular cytoskeleton, we performed western blots for cytoplasmic dynein and kinesin heavy chain using the same brain tissue samples from 30 days old WT and  $\alpha$ -adducin KO animals as used for the analysis of tubulin PTMs. Since axonal transport velocity is decreased in the absence of adducin, it was predictable that both molecular motors could also have reduced levels when compared with those present in WT animals. As predicted,  $\alpha$ -adducin KO mice had a severe statistical decline in the levels of both cytoplasmic dynein and kinesin heavy chain (figure 21).

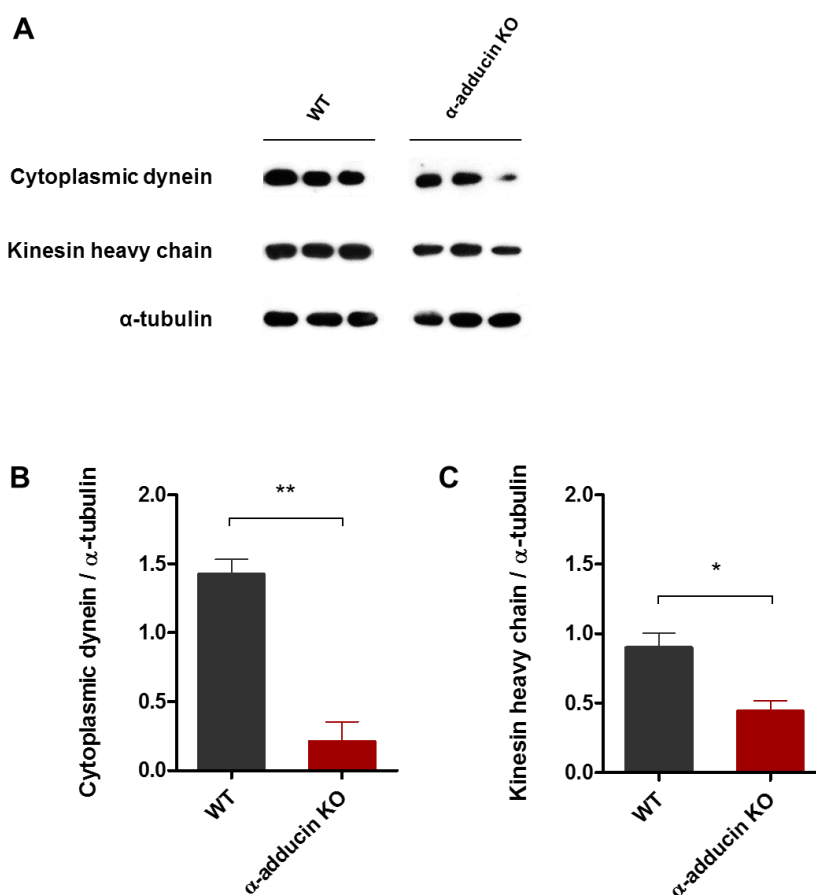


**Figure 21 – Analysis of the levels of molecular motors in WT and  $\alpha$ -adducin KO mouse brains.** (A) Representative Western blot. (B-C) Quantification of the levels of (B) cytoplasmic dynein and (C) kinesin heavy chain in brain tissue samples from  $\alpha$ -adducin KO and WT P30 mice. Graphs show mean  $\pm$  SEM; p-value  $<0.05$ ,  $**<0.01$ .

## V. The lack of adducin impairs the plasticity of the axon initial segment.

The Axon Initial Segment is an actin-enriched axon domain dependent on high densities of voltage gated sodium channels. Chronic depolarization of neurons is known to generate a distal relocation of the AIS such that the neuronal excitability is restored [37-39, 45, 46]. As mentioned before, actin is enriched in the AIS and the actin cytoskeleton can influence the precise location of the AIS within the axon and also its plasticity [48].

Here we aimed at understanding the role of adducin in AIS plasticity given that the lack of adducin is associated with a more unstable actin cytoskeleton. To test the hypothesis that adducin might be involved in the formation and/or plasticity of the AIS, we used cultures of embryonic hippocampal neurons of WT and  $\alpha$ -adducin KO mice and submitted them to high levels of potassium in order to promote a chronic depolarization. When WT neurons were submitted to depolarization by increased extracellular potassium levels, the AIS moved forward. In WT animals both the start and the end of the AIS moved resulting in AIS relocation (figure 22A). In contrast, in  $\alpha$ -adducin KO animals, the plasticity of the AIS was impaired and no movement was observed upon chronic depolarization (figure 22A). When  $\alpha$ -adducin KO neurons were depolarized, the start of the AIS hardly moved and the end of the AIS not only did not move as it seemed to regress (figure 22B).

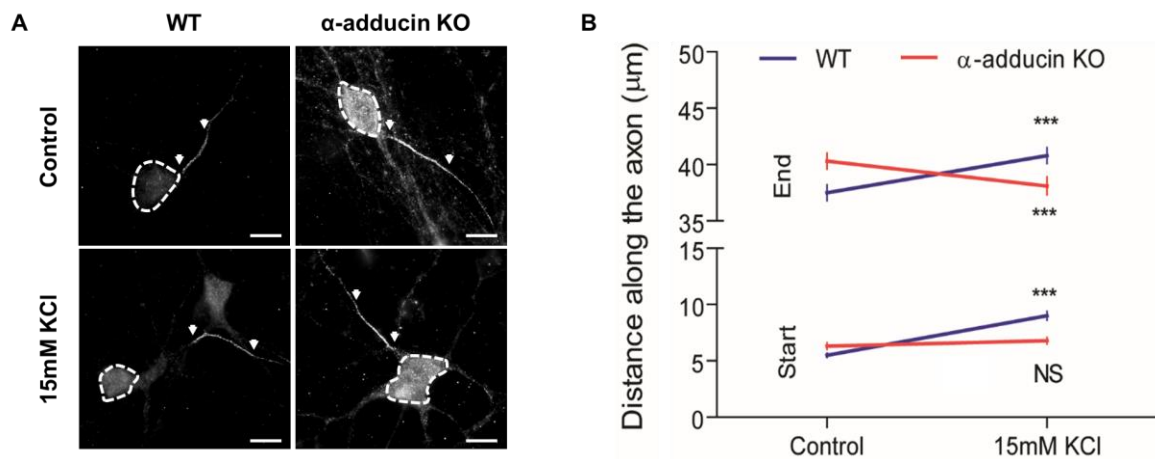


**Figure 22 – Analysis of the AIS plasticity in WT and  $\alpha$ -adducin KO embryonic hippocampal neurons.**

(A) Representative images of the immunofluorescence against ankyrinG in WT and  $\alpha$ -adducin KO hippocampal neurons either under control conditions or after chronic depolarization induced by 15mM KCl; scale bar: 10  $\mu$ m. Cell bodies are surrounded by a white dashed line. The AIS is highlighted by arrowheads. (B) Analysis of the distance along the axon of the start and the end of the AIS in WT and  $\alpha$ -adducin KO hippocampal neurons either under control conditions or after chronic depolarization induced by 15mM KCl. Graphs show mean  $\pm$  SEM; p-value  $*** < 0.001$ .

In summary,  $\alpha$ -adducin KO embryonic hippocampal neurons do not have the ability to relocate the AIS in response to cell electrical changes. These results support the initial hypothesis of the crucial role of adducin, an actin capping protein, in the maintenance of the actin cytoskeleton organization which includes an efficient axon initial segment plasticity.

Part of the Results presented in this thesis have been incorporated in a manuscript (Leite SC, Sampaio P, Sousa VF, **Nogueira-Rodrigues J**, Costa R, Peters LL, Brites P and Sousa MM. The actin-binding protein  $\alpha$ -adducin is required for maintaining axon diameter) that has recently been submitted to publication.

## Discussion

The neuronal cytoskeleton is a tightly regulated structure where the interplay of its three main components, actin, microtubules and neurofilaments is crucial. With the discovery of axon actin rings, the neuronal actin cytoskeleton has gained relevance. Still, the molecular details of the regulation of the actin cytoskeleton in neurons are largely unknown.

Similarly to what happens in erythrocytes [87], in the nervous system, we show that depletion of  $\alpha$  subunit of adducin results in an almost absence of both the  $\beta$  and  $\gamma$  isoforms. As a consequence, no functional adducin tetramer complex is formed. Although  $\alpha$ -adducin KO mice lack functional adducin, capping protein CapZ were found in similar levels to those present in WT animals which suggest there is no compensation by other actin capping proteins.

Given that the lack of adducin in the nervous system results in axon enlargement and axonal loss (both in the CNS and PNS), we evaluated a possible effect in axonal transport as disruptions in axonal transport may be an important cause of neurodegeneration [59, 60, 63, 64, 101-104]. Although no differences were found in the transport of cholera toxin in the optic nerve, probably given the low sensitivity of this method, the lack of adducin resulted in a decreased speed of axonal transport of mitochondria and lysosomes despite that in the case of synaptic vesicles, no differences in the speed of transport were found. Actually, the reason why only the transport of organelles is affected (and not that of synaptic vesicles) could be related with the different sizes of these moving cargos or even with their different binding associated-proteins. We know that in  $\alpha$ -adducin KO neurons there is axonal enlargement, but a possible connection between the increase in axonal diameter and the decreased speed of axonal transport, remains to be demonstrated. In fact, the rate of fast axonal transport is thought to be independent of axon caliber [121, 122]. Still, the causes behind the decreased velocity of axonal transport of mitochondria and lysosomes in  $\alpha$ -adducin KO neurons remains vague.

Microtubules (MTs) are particularly important to the neuronal cytoskeleton being involved in several neuron cell processes including mitosis, cell motility, axonal transport, cell morphology and neuronal polarization [1, 2, 14]. In this respect it is interesting to note that  $\alpha$ -adducin interacts with MTs via myosin X [123]. Axonal transport can be directly regulated by the MT cytoskeleton [124] since MTs can form tracks along the axon allowing

an efficient transport of various cargos by the appropriate association with the motor proteins, like kinesin and dynein [63] that can move directionally along MTs, facilitating the long-range transport into distal axons and dendrites [124]. There are some regulators of MTs that can modulate their functionalities namely the post-translational modifications (PTM) of tubulin [125]. PTMs of tubulin might be involved in the recruitment of specific proteins regulating MT properties [118] including the transport along the axon having an important role in MT dynamics and motor traffic. Moreover, several neurodegenerative disorders have been associated with axonal transport deficits and, consequently, with alterations in MT-based transport [125]. In this thesis, we focused on three tubulin modifications: acetylation, tyrosination and de-tyrosination. Although no differences were found in the levels of acetylated and de-tyrosinated tubulin, the levels of tyrosinated tubulin were significantly decreased when comparing WT and  $\alpha$ -adducin KO brains. It is known that increased levels of tubulin tyrosination and, consequently, more tyrosine being added to the plus end of MTs are indicative of a more dynamic state of the cytoskeleton [118-120]. Given that the levels of tubulin tyrosination were reduced in  $\alpha$ -adducin KOs, we can assume that there is a less dynamic status of the microtubule cytoskeleton in the  $\alpha$ -adducin KO mice. Whether there is some direct relation between adducin and tubulin tyrosination, or decreased tubulin tyrosination and axonal transport remains to be further explored.

Axonal transport can be also affected by molecular motors, dynein and kinesin, that can be regulated via MT PTMs [119]. In fact, the cycle de-tyrosination/tyrosination of tubulin recruits the motor protein kinesin that binds preferentially to de-tyrosinated microtubules rather than tyrosinated ones [126]. Furthermore, acetylation of tubulin has been associated with an increase in MT binding of both kinesin and dynein [127, 128]. Besides differential PTMs of tubulin the decreased axonal transport speed may result from an excessive attachment of MT-associated proteins that may compete with molecular motors inhibiting their binding to MTs [129], resulting in a decrease in the levels of MT-bound dynein and kinesin in  $\alpha$ -adducin KO mice.

Finally, in this work we aimed at comprehending the importance of adducin in another important aspect of neuron biology that is the plasticity of the axon initial segment. It is not fully understood how AIS plasticity is regulated but actin is required for the AIS formation and also for establishing the AIS barrier [50]. Using *in vitro* cultures of embryonic hippocampal neurons, we observed that in  $\alpha$ -adducin KO animals, although the AIS forms normally, neurons do not have the ability to relocate it in response to chronic depolarization. These results support the hypothesis that adducin might be involved in the

organization and/or plasticity of the AIS. Interestingly, adducin is regulated by PKC [78, 88] which requires increased calcium levels to be activated and calcium signaling is fundamental for AIS relocation [39]. Alternatively, the effect of adducin on AIS plasticity may be the consequence of dysregulation of voltage-gated ion channels, as in other biological systems adducin binds Na/K pumps [130], regulating their endocytosis [131]. Although we know that the actin cytoskeleton dynamics contributes to AIS maintenance, the specific role of actin and its associated proteins, like adducin, in this process remains unclear.

In sum, with this Thesis we contributed to understand the relevance of the actin-binding protein adducin in neuron biology.

## References

1. Fletcher, D.A. and R.D. Mullins, *Cell mechanics and the cytoskeleton*. Nature, 2010. **463**(7280): p. 485-92.
2. Stuessi, M. and F. Bradke, *Neuronal polarization: the cytoskeleton leads the way*. Dev Neurobiol, 2011. **71**(6): p. 430-44.
3. Pollard, T.D. and J.A. Cooper, *Actin, a central player in cell shape and movement*. Science, 2009. **326**(5957): p. 1208-12.
4. Sunkel, C. and C. Azevedo, *Biologia Molecular e Celular*. 5ª edição ed. 2012, Lisboa: LIDEL.
5. Sainath, R. and G. Gallo, *Cytoskeletal and signaling mechanisms of neurite formation*. Cell Tissue Res, 2015. **359**(1): p. 267-78.
6. Bradke, F. and C.G. Dotti, *The role of local actin instability in axon formation*. Science, 1999. **283**(5409): p. 1931-1934.
7. Lee, S.H. and R. Dominguez, *Regulation of actin cytoskeleton dynamics in cells*. Mol Cells, 2010. **29**(4): p. 311-25.
8. McMurray, C.T., *Neurodegeneration: diseases of the cytoskeleton?* Cell Death Differ, 2000. **7**(10): p. 861-5.
9. Bradke, F. and C.G. Dotti, *Establishment of neuronal polarity: lessons from cultured hippocampal neurons*. Curr Opin Neurobiol, 2000. **10**(5): p. 574-81.
10. Witte, H. and F. Bradke, *The role of the cytoskeleton during neuronal polarization*. Curr Opin Neurobiol, 2008. **18**(5): p. 479-87.
11. Yoshimura, T., N. Arimura, and K. Kaibuchi, *Signaling networks in neuronal polarization*. J Neurosci, 2006. **26**(42): p. 10626-30.
12. Dotti, C.G., C.A. Sullivan, and G.A. Banker, *The establishment of polarity by hippocampal neurons in culture*. J Neurosci, 1988. **8**(4): p. 1454-68.
13. Goslin, K. and G. Banker, *Experimental observations on the development of polarity by hippocampal neurons in culture*. J Cell Biol, 1989. **108**(4): p. 1507-16.
14. Neukirchen, D. and F. Bradke, *Neuronal polarization and the cytoskeleton*. Semin Cell Dev Biol, 2011. **22**(8): p. 825-33.
15. Barnes, A.P. and F. Polleux, *Establishment of axon-dendrite polarity in developing neurons*. Annu Rev Neurosci, 2009. **32**: p. 347-81.
16. Tahirovic, S. and F. Bradke, *Neuronal polarity*. Cold Spring Harb Perspect Biol, 2009. **1**(3): p. a001644.

17. Gomis-Ruth, S., C.J. Wierenga, and F. Bradke, *Plasticity of polarization: changing dendrites into axons in neurons integrated in neuronal circuits*. *Curr Biol*, 2008. **18**(13): p. 992-1000.
18. Andersen, S.S. and G.Q. Bi, *Axon formation: a molecular model for the generation of neuronal polarity*. *Bioessays*, 2000. **22**(2): p. 172-9.
19. Gomez, T.M. and P.C. Letourneau, *Actin dynamics in growth cone motility and navigation*. *J Neurochem*, 2014. **129**(2): p. 221-34.
20. Gallo, G., *Mechanisms underlying the initiation and dynamics of neuronal filopodia: from neurite formation to synaptogenesis*. *Int Rev Cell Mol Biol*, 2013. **301**: p. 95-156.
21. Gallo, G. and L. Lanier, *Neurobiology of Actin: From Neurulation to Synaptic Function*. Vol. 5. 2011: Springer New York.
22. Lowery, L.A. and D. Van Vactor, *The trip of the tip: understanding the growth cone machinery*. *Nat Rev Mol Cell Biol*, 2009. **10**(5): p. 332-43.
23. Vitriol, E.A. and J.Q. Zheng, *Growth cone travel in space and time: the cellular ensemble of cytoskeleton, adhesion, and membrane*. *Neuron*, 2012. **73**(6): p. 1068-81.
24. Neukirchen, D. and F. Bradke, *Cytoplasmic linker proteins regulate neuronal polarization through microtubule and growth cone dynamics*. *J Neurosci*, 2011. **31**(4): p. 1528-38.
25. Pak, C.W., K.C. Flynn, and J.R. Bamberg, *Actin-binding proteins take the reins in growth cones*. *Nat Rev Neurosci*, 2008. **9**(2): p. 136-47.
26. Goncalves-Pimentel, C., et al., *Dissecting regulatory networks of filopodia formation in a Drosophila growth cone model*. *PLoS One*, 2011. **6**(3): p. e18340.
27. Lee, C.W., et al., *Dynamic localization of G-actin during membrane protrusion in neuronal motility*. *Curr Biol*, 2013. **23**(12): p. 1046-56.
28. Kovar, D.R., et al., *Control of the assembly of ATP- and ADP-actin by formins and profilin*. *Cell*, 2006. **124**(2): p. 423-35.
29. Sarmiere, P.D. and J.R. Bamberg, *Regulation of the neuronal actin cytoskeleton by ADF/cofilin*. *J Neurobiol*, 2004. **58**(1): p. 103-17.
30. Krause, M., et al., *Ena/VASP proteins: regulators of the actin cytoskeleton and cell migration*. *Annu Rev Cell Dev Biol*, 2003. **19**: p. 541-64.
31. Takenawa, T. and S. Suetsugu, *The WASP-WAVE protein network: connecting the membrane to the cytoskeleton*. *Nat Rev Mol Cell Biol*, 2007. **8**(1): p. 37-48.



32. Rasband, M.N., *The axon initial segment and the maintenance of neuronal polarity*. Nat Rev Neurosci, 2010. **11**(8): p. 552-62.
33. Yoshimura, T. and M.N. Rasband, *Axon initial segments: diverse and dynamic neuronal compartments*. Curr Opin Neurobiol, 2014. **27**: p. 96-102.
34. Hedstrom, K.L., et al., *Neurofascin assembles a specialized extracellular matrix at the axon initial segment*. J Cell Biol, 2007. **178**(5): p. 875-86.
35. Bender, K.J. and L.O. Trussell, *The physiology of the axon initial segment*. Annu Rev Neurosci, 2012. **35**: p. 249-65.
36. Kole, M.H. and G.J. Stuart, *Signal processing in the axon initial segment*. Neuron, 2012. **73**(2): p. 235-47.
37. Kole, M.H., et al., *Action potential generation requires a high sodium channel density in the axon initial segment*. Nat Neurosci, 2008. **11**(2): p. 178-86.
38. Kole, M.H., J.J. Letzkus, and G.J. Stuart, *Axon initial segment Kv1 channels control axonal action potential waveform and synaptic efficacy*. Neuron, 2007. **55**(4): p. 633-47.
39. Grubb, M.S. and J. Burrone, *Activity-dependent relocation of the axon initial segment fine-tunes neuronal excitability*. Nature, 2010. **465**(7301): p. 1070-4.
40. Fatt, P., *Sequence of events in synaptic activation of a motoneurone*. J Neurophysiol, 1957. **20**(1): p. 61-80.
41. Galiano, M.R., et al., *A distal axonal cytoskeleton forms an intra-axonal boundary that controls axon initial segment assembly*. Cell, 2012. **149**(5): p. 1125-39.
42. Hedstrom, K.L., Y. Ogawa, and M.N. Rasband, *AnkyrinG is required for maintenance of the axon initial segment and neuronal polarity*. J Cell Biol, 2008. **183**(4): p. 635-40.
43. Garrido, J.J., et al., *A targeting motif involved in sodium channel clustering at the axonal initial segment*. Science, 2003. **300**(5628): p. 2091-4.
44. Rasmussen, H.B., et al., *Requirement of subunit co-assembly and ankyrin-G for M-channel localization at the axon initial segment*. J Cell Sci, 2007. **120**(Pt 6): p. 953-63.
45. Buffington, S.A. and M.N. Rasband, *The axon initial segment in nervous system disease and injury*. Eur J Neurosci, 2011. **34**(10): p. 1609-19.
46. Kuba, H., Y. Oichi, and H. Ohmori, *Presynaptic activity regulates Na(+) channel distribution at the axon initial segment*. Nature, 2010. **465**(7301): p. 1075-8.
47. Sobotzik, J.M., et al., *AnkyrinG is required to maintain axo-dendritic polarity in vivo*. Proc Natl Acad Sci U S A, 2009. **106**(41): p. 17564-9.

48. Jones, S.L., F. Korobova, and T. Svitkina, *Axon initial segment cytoskeleton comprises a multiprotein submembranous coat containing sparse actin filaments*. J Cell Biol, 2014. **205**(1): p. 67-81.
49. Al-Bassam, S., et al., *Differential trafficking of transport vesicles contributes to the localization of dendritic proteins*. Cell Rep, 2012. **2**(1): p. 89-100.
50. Watanabe, K., et al., *Networks of polarized actin filaments in the axon initial segment provide a mechanism for sorting axonal and dendritic proteins*. Cell Rep, 2012. **2**(6): p. 1546-53.
51. Nakada, C., et al., *Accumulation of anchored proteins forms membrane diffusion barriers during neuronal polarization*. Nat Cell Biol, 2003. **5**(7): p. 626-32.
52. Song, A.H., et al., *A selective filter for cytoplasmic transport at the axon initial segment*. Cell, 2009. **136**(6): p. 1148-60.
53. Xu, K., G. Zhong, and X. Zhuang, *Actin, spectrin, and associated proteins form a periodic cytoskeletal structure in axons*. Science, 2013. **339**(6118): p. 452-6.
54. Gallo, G., *More than one ring to bind them all: recent insights into the structure of the axon*. Dev Neurobiol, 2013. **73**(11): p. 799-805.
55. Zhong, G., et al., *Developmental mechanism of the periodic membrane skeleton in axons*. Elife, 2014. **3**.
56. Hammarlund, M., E.M. Jorgensen, and M.J. Bastiani, *Axons break in animals lacking beta-spectrin*. J Cell Biol, 2007. **176**(3): p. 269-75.
57. Pielage, J., R.D. Fetter, and G.W. Davis, *Presynaptic spectrin is essential for synapse stabilization*. Curr Biol, 2005. **15**(10): p. 918-28.
58. D'Este, E., et al., *STED nanoscopy reveals the ubiquity of subcortical cytoskeleton periodicity in living neurons*. Cell Rep, 2015. **10**(8): p. 1246-51.
59. Morfini, G., et al., *Axonal Transport*, in *Basic Neurochemistry: Principles of Molecular, Cellular and Medical Neurobiology*. 2011, Elsevier. p. 146-164.
60. Duncan, J.E. and L.S. Goldstein, *The genetics of axonal transport and axonal transport disorders*. PLoS Genet, 2006. **2**(9): p. e124.
61. Lasek, R.J., J.A. Garner, and S.T. Brady, *Axonal transport of the cytoplasmic matrix*. J Cell Biol, 1984. **99**(1 Pt 2): p. 212s-221s.
62. Hirokawa, N., S. Niwa, and Y. Tanaka, *Molecular motors in neurons: transport mechanisms and roles in brain function, development, and disease*. Neuron, 2010. **68**(4): p. 610-38.
63. Millecamps, S. and J.P. Julien, *Axonal transport deficits and neurodegenerative diseases*. Nat Rev Neurosci, 2013. **14**(3): p. 161-76.

64. Chevalier-Larsen, E. and E. Holzbaur, *Axonal transport and neurodegenerative disease*. Biochimica et Biophysica Acta, 2006. **1762**: p. 1094-1108.
65. Baas, P.W. and D.W. Buster, *Slow axonal transport and the genesis of neuronal morphology*. J Neurobiol, 2004. **58**(1): p. 3-17.
66. Hirokawa, N. and R. Takemura, *Molecular motors in neuronal development, intracellular transport and diseases*. Current Opinion in Neurobiology, 2004. **14**: p. 564-573.
67. Vale, R., T. Reese, and M. Sheetz, *Identification of a novel force-generating protein, kinesin, involved in microtubule-based motility*. Cell, 1985. **42**(1): p. 39-50.
68. Eschbach, J. and L. Dupuis, *Cytoplasmic dynein in neurodegeneration*. Pharmacol Ther, 2011. **130**(3): p. 348-63.
69. Bennett, V., *Spectrin-based membrane skeleton: a multipotential adaptor between plasma membrane and cytoplasm*. Physiol Rev, 1990. **70**(4): p. 1029-65.
70. Bennett, V. and D.M. Gilligan, *The spectrin-based membrane skeleton and micron-scale organization of the plasma membrane*. Annu Rev Cell Biol, 1993. **9**: p. 27-66.
71. Li, X. and V. Bennett, *Identification of the spectrin subunit and domains required for formation of spectrin/adducin/actin complexes*. J Biol Chem, 1996. **271**(26): p. 15695-702.
72. Bennett, V. and A.J. Baines, *Spectrin and ankyrin-based pathways: metazoan inventions for integrating cells into tissues*. Physiol Rev, 2001. **81**(3): p. 1353-92.
73. Baines, A.J., *Evolution of spectrin function in cytoskeletal and membrane networks*. Biochem Soc Trans, 2009. **37**(Pt 4): p. 796-803.
74. Naydenov, N.G. and A.I. Ivanov, *Spectrin-adducin membrane skeleton: A missing link between epithelial junctions and the actin cytoskeleton?* Bioarchitecture, 2011. **1**(4): p. 186-191.
75. Matsuoka, Y., X. Li, and V. Bennett, *Adducin: structure, function and regulation*. Cell Mol Life Sci, 2000. **57**(6): p. 884-95.
76. Li, X., Y. Matsuoka, and V. Bennett, *Adducin preferentially recruits spectrin to the fast growing ends of actin filaments in a complex requiring the MARCKS-related domain and a newly defined oligomerization domain*. J Biol Chem, 1998. **273**(30): p. 19329-38.
77. Ling, E., K. Gardner, and V. Bennett, *Protein kinase C phosphorylates a recently identified membrane skeleton-associated calmodulin-binding protein in human erythrocytes*. J Biol Chem, 1986. **261**(30): p. 13875-8.

78. Matsuoka, Y., C.A. Hughes, and V. Bennett, *Adducin regulation. Definition of the calmodulin-binding domain and sites of phosphorylation by protein kinases A and C*. J Biol Chem, 1996. **271**(41): p. 25157-66.
79. Dong, L., et al., *35H, a sequence isolated as a protein kinase C binding protein, is a novel member of the adducin family*. J Biol Chem, 1995. **270**(43): p. 25534-40.
80. Joshi, R., et al., *Primary structure and domain organization of human alpha and beta adducin*. J Cell Biol, 1991. **115**(3): p. 665-75.
81. Gilligan, D.M., et al., *Targeted disruption of the beta adducin gene (Add2) causes red blood cell spherocytosis in mice*. Proc Natl Acad Sci U S A, 1999. **96**(19): p. 10717-22.
82. Bennett, V., K. Gardner, and J.P. Steiner, *Brain adducin: a protein kinase C substrate that may mediate site-directed assembly at the spectrin-actin junction*. J Biol Chem, 1988. **263**(12): p. 5860-9.
83. Joshi, R. and V. Bennett, *Mapping the domain structure of human erythrocyte adducin*. J Biol Chem, 1990. **265**(22): p. 13130-6.
84. Hughes, C.A. and V. Bennett, *Adducin: a physical model with implications for function in assembly of spectrin-actin complexes*. J Biol Chem, 1995. **270**(32): p. 18990-6.
85. Baines, A.J., *The spectrin-ankyrin-4.1-adducin membrane skeleton: adapting eukaryotic cells to the demands of animal life*. Protoplasma, 2010. **244**(1-4): p. 99-131.
86. Stevens, R.J. and J.T. Littleton, *Synaptic growth: dancing with adducin*. Curr Biol, 2011. **21**(10): p. R402-5.
87. Robledo, R.F., et al., *Targeted deletion of alpha-adducin results in absent beta- and gamma-adducin, compensated hemolytic anemia, and lethal hydrocephalus in mice*. Blood, 2008. **112**(10): p. 4298-307.
88. Matsuoka, Y., X. Li, and V. Bennett, *Adducin is an in vivo substrate for protein kinase C: phosphorylation in the MARCKS-related domain inhibits activity in promoting spectrin-actin complexes and occurs in many cells, including dendritic spines of neurons*. J Cell Biol, 1998. **142**(2): p. 485-97.
89. Zhao, K.N., P.P. Masci, and M.F. Lavin, *Disruption of spectrin-like cytoskeleton in differentiating keratinocytes by PKCdelta activation is associated with phosphorylated adducin*. PLoS One, 2011. **6**(12): p. e28267.
90. Lavaur, J., Y.S. Mineur, and M.R. Picciotto, *The membrane cytoskeletal protein adducin is phosphorylated by protein kinase C in D1 neurons of the nucleus*

- accumbens and dorsal striatum following cocaine administration.* J Neurochem, 2009. **111**(5): p. 1129-37.
91. Chen, C.L., Y.T. Hsieh, and H.C. Chen, *Phosphorylation of adducin by protein kinase Cdelta promotes cell motility.* J Cell Sci, 2007. **120**(Pt 7): p. 1157-67.
  92. Lin, H., L. Yue, and A.C. Spradling, *The Drosophila fusome, a germline-specific organelle, contains membrane skeletal proteins and functions in cyst formation.* Development, 1994. **120**(4): p. 947-56.
  93. Yue, L. and A.C. Spradling, *hu-li tai shao, a gene required for ring canal formation during Drosophila oogenesis, encodes a homolog of adducin.* Genes Dev, 1992. **6**(12B): p. 2443-54.
  94. Whittaker, K.L., et al., *Different 3' untranslated regions target alternatively processed hu-li tai shao (hts) transcripts to distinct cytoplasmic locations during Drosophila oogenesis.* J Cell Sci, 1999. **112 ( Pt 19)**: p. 3385-98.
  95. Petrella, L.N., T. Smith-Leiker, and L. Cooley, *The Ovhts polyprotein is cleaved to produce fusome and ring canal proteins required for Drosophila oogenesis.* Development, 2007. **134**(4): p. 703-12.
  96. Pielage, J., et al., *Hts/Adducin controls synaptic elaboration and elimination.* Neuron, 2011. **69**(6): p. 1114-31.
  97. Robinson, D.N., K. Cant, and L. Cooley, *Morphogenesis of Drosophila ovarian ring canals.* Development, 1994. **120**(7): p. 2015-25.
  98. Kuhlman, P.A., et al., *A new function for adducin. Calcium/calmodulin-regulated capping of the barbed ends of actin filaments.* J Biol Chem, 1996. **271**(14): p. 7986-91.
  99. Derick, L.H., et al., *Protein immunolocalization in the spread erythrocyte membrane skeleton.* Eur J Cell Biol, 1992. **57**(2): p. 317-20.
  100. Gardner, K. and V. Bennett, *Modulation of spectrin-actin assembly by erythrocyte adducin.* Nature, 1987. **328**(6128): p. 359-62.
  101. Baloh, R.H., et al., *Altered axonal mitochondrial transport in the pathogenesis of Charcot-Marie-Tooth disease from mitofusin 2 mutations.* J Neurosci, 2007. **27**(2): p. 422-30.
  102. Ebbing, B., et al., *Effect of spastic paraplegia mutations in KIF5A kinesin on transport activity.* Hum Mol Genet, 2008. **17**(9): p. 1245-52.
  103. Hurd, D.D., M. Stern, and W.M. Saxton, *Mutation of the axonal transport motor kinesin enhances paralytic and suppresses Shaker in Drosophila.* Genetics, 1996. **142**(1): p. 195-204.

104. LaMonte, B.H., et al., *Disruption of dynein/dynactin inhibits axonal transport in motor neurons causing late-onset progressive degeneration*. *Neuron*, 2002. **34**(5): p. 715-27.
105. Abbott, C.J., et al., *Imaging axonal transport in the rat visual pathway*. *Biomed Opt Express*, 2013. **4**(2): p. 364-86.
106. Conte, W.L., H. Kamishina, and R.L. Reep, *Multiple neuroanatomical tract-tracing using fluorescent Alexa Fluor conjugates of cholera toxin subunit B in rats*. *Nat Protoc*, 2009. **4**(8): p. 1157-66.
107. Fleming, M.D., R.M. Benca, and M. Behan, *Retinal projections to the subcortical visual system in congenic albino and pigmented rats*. *Neuroscience*, 2006. **143**(3): p. 895-904.
108. Lencer, W.I., *Retrograde transport of cholera toxin into the ER of host cells*. *Int J Med Microbiol*, 2004. **293**(7-8): p. 491-4.
109. Luppi, P.H., P. Fort, and M. Jouvet, *Iontophoretic application of unconjugated cholera toxin B subunit (CTb) combined with immunohistochemistry of neurochemical substances: a method for transmitter identification of retrogradely labeled neurons*. *Brain Res*, 1990. **534**(1-2): p. 209-24.
110. Reuss, S. and K. Decker, *Anterograde tracing of retinohypothalamic afferents with Fluoro-Gold*. *Brain Res*, 1997. **745**(1-2): p. 197-204.
111. Sun, J.B., J. Holmgren, and C. Czerkinsky, *Cholera toxin B subunit: an efficient transmucosal carrier-delivery system for induction of peripheral immunological tolerance*. *Proc Natl Acad Sci U S A*, 1994. **91**(23): p. 10795-9.
112. Trojanowski, J.Q., J.O. Gonatas, and N.K. Gonatas, *Horseradish peroxidase (HRP) conjugates of cholera toxin and lectins are more sensitive retrogradely transported markers than free HRP*. *Brain Res*, 1982. **231**(1): p. 33-50.
113. Wan, X.C., J.Q. Trojanowski, and J.O. Gonatas, *Cholera toxin and wheat germ agglutinin conjugates as neuroanatomical probes: their uptake and clearance, transganglionic and retrograde transport and sensitivity*. *Brain Res*, 1982. **243**(2): p. 215-24.
114. Wu, C.C., R.M. Russell, and H.J. Karten, *The transport rate of cholera toxin B subunit in the retinofugal pathways of the chick*. *Neuroscience*, 1999. **92**(2): p. 665-76.
115. Wu, C.C., et al., *Tracing developing pathways in the brain: a comparison of carbocyanine dyes and cholera toxin b subunit*. *Neuroscience*, 2003. **117**(4): p. 831-45.

116. Tong, Y.G., et al., *Increased uptake and transport of cholera toxin B-subunit in dorsal root ganglion neurons after peripheral axotomy: possible implications for sensory sprouting*. J Comp Neurol, 1999. **404**(2): p. 143-58.
117. Baas, P.W., C. Vidya Nadar, and K.A. Myers, *Axonal transport of microtubules: the long and short of it*. Traffic, 2006. **7**(5): p. 490-8.
118. Hammond, J.W., D. Cai, and K.J. Verhey, *Tubulin modifications and their cellular functions*. Curr Opin Cell Biol, 2008. **20**(1): p. 71-6.
119. Janke, C. and J.C. Bulinski, *Post-translational regulation of the microtubule cytoskeleton: mechanisms and functions*. Nat Rev Mol Cell Biol, 2011. **12**(12): p. 773-86.
120. Janke, C., *The tubulin code: molecular components, readout mechanisms, and functions*. J Cell Biol, 2014. **206**(4): p. 461-72.
121. Ochs, S., *Rate of fast axoplasmic transport in mammalian nerve fibres*. J Physiol, 1972. **227**(3): p. 627-45.
122. Wortman, J.C., et al., *Axonal transport: how high microtubule density can compensate for boundary effects in small-caliber axons*. Biophys J, 2014. **106**(4): p. 813-23.
123. Chan, P.C., et al., *Adducin-1 is essential for mitotic spindle assembly through its interaction with myosin-X*. J Cell Biol, 2014. **204**(1): p. 19-28.
124. Franker, M.A. and C.C. Hoogenraad, *Microtubule-based transport - basic mechanisms, traffic rules and role in neurological pathogenesis*. J Cell Sci, 2013. **126**(Pt 11): p. 2319-29.
125. Janke, C. and M. Kneussel, *Tubulin post-translational modifications: encoding functions on the neuronal microtubule cytoskeleton*. Trends Neurosci, 2010. **33**(8): p. 362-72.
126. Liao, G. and G.G. Gundersen, *Kinesin is a candidate for cross-bridging microtubules and intermediate filaments. Selective binding of kinesin to detyrosinated tubulin and vimentin*. J Biol Chem, 1998. **273**(16): p. 9797-803.
127. Dompierre, J.P., et al., *Histone deacetylase 6 inhibition compensates for the transport deficit in Huntington's disease by increasing tubulin acetylation*. J Neurosci, 2007. **27**(13): p. 3571-83.
128. Reed, N.A., et al., *Microtubule acetylation promotes kinesin-1 binding and transport*. Curr Biol, 2006. **16**(21): p. 2166-72.
129. Dixit, R., et al., *Differential regulation of dynein and kinesin motor proteins by tau*. Science, 2008. **319**(5866): p. 1086-9.

130. Gallardo, G., et al., *An alpha2-Na/K ATPase/alpha-adducin complex in astrocytes triggers non-cell autonomous neurodegeneration*. Nat Neurosci, 2014. **17**(12): p. 1710-9.
131. Torielli, L., et al., *alpha-Adducin mutations increase Na/K pump activity in renal cells by affecting constitutive endocytosis: implications for tubular Na reabsorption*. Am J Physiol Renal Physiol, 2008. **295**(2): p. F478-87.